2008

Molecular Genetic Approaches to Disease of Neural Development

Mohamad Bydon
Yale University

MOLECULAR GENETIC APPROACHES TO DISEASES OF NEURAL DEVELOPMENT

A Thesis Submitted to the

Yale University School of Medicine

in Partial Fulfillment of the Requirements for the

Degree of Doctor of Medicine

by

Mohamad Bydon

2008

ABSTRACT

MOLECULAR GENETIC APPROACHES TO DISEASES OF NEURAL DEVELOPMENT.

Mohamad Bydon, Kaya Bilguvar, Fatih Bayrakli, Luis Kolb, and Murat Gunel.

Department of Neurosurgery, Yale University School of Medicine, New Haven, CT.

This study utilized novel genetic techniques in order to find causative gene mutations that underlie diseases of neural development. Our laboratory has collected 175 cases of malformations of cortical development (MCD) from the United States and Europe. Four of these cases are the focus of this manuscript: two familial cases of infantile neuroaxonal dystrophy (INAD), a familial case of hereditary spastic paraparesis (HSP), and a sporadic case of Greig cephalopolysyndactyly (GCPS) and cerebral cavernous malformations (CCMs).

The techniques utilized to study the affected patients include microarray-based single nucleotide polymorphism (SNP) genotyping and copy number variation (CNV) analysis, both of which are powerful tools in the hunt for disease-causing gene mutations.

In the familial cases of INAD, we report two novel mutations in the *PLA2G6* gene, previously shown to cause INAD when mutated. In the familial case of HSP, we demonstrate linkage to the SPG11 locus on chromosome 15q. Finally, in the sporadic

case of GCPS and CCM, we published the first report on this novel syndrome along with a genetic analysis that demonstrates a microdeletion on chromosome 7p, resulting in heterozygous loss of both the *GLI3* and *CCM2* genes.

The three studies presented in this manuscript demonstrate the utility of SNP genotyping and CNV analysis in revealing the genetic mutations that underlie diseases of neural development.

ACKNOWLEDGMENTS

I wish to thank my mentor Murat Gunel for his advice, support, and guidance throughout the past four years.

I wish to thank Kaya Bilguvar, Fatih Bayrakli, and Chris Mason for their significant contributions to this manuscript.

I wish to thank Angiliki Louvi for her helpful commentary and corrections through the many revisions of this work.

I wish to thank my parents and siblings for all their help and support. I wish to thank Salma for her devotion, her endless motivation, and her willingness to see me through any undertaking.

This project was funded by the NIH and the Program on Neurogenetics at Yale University School of Medicine.

TABLE OF CONTENTS

INTRODUCTION

While humans share 99% of their DNA sequences, there are many examples of genetic variation in the genome, ranging from large chromosomal abnormalities to insertions or deletions of one or more nucleotides. It is believed that within the 3 billion bases of the human genome, there are more than 10 million common nucleotide variations between individuals (1). A single nucleotide variation occurs when a nucleotide – A, C, T, or G – in an individual's DNA is altered. For this variation to be considered a single nucleotide polymorphism (SNP), it must occur in 1% of the population. The International Haplotype Mapping Project (2) has identified more than 2 million SNP markers, which can be used in large-scale genotyping.

SNPs, as well as other genetic variations, have become of great interest to the scientific community because they are thought to predispose individuals to disease (3, 4). Advances in SNP genotyping have been made possible by the development of microarrays, membranes or glass slides on which probes – sequences of DNA – are fixed in an orderly arrangement. Microarrays facilitate the detection of thousands of genomic variants, including SNPs and more recently copy number variations, in a sample simultaneously. Microarray-based methods for SNP genotyping (5) have been used in linkage and association studies of complex disorders such as prostate cancer (6), rheumatoid arthritis (7), erythrokeratodermia variabilis (8), bladder cancer (9), systemic lupus erythematosus (10), and dyslipidemia (11) (Table 3).

In addition to their utilization in SNP genotyping, microarray-based methods have been used in the analysis of copy number variations (CNVs) spanning large chromosomal regions (12). Sebat et al. (13) recently demonstrated the presence of CNVs, DNA segments found throughout the human genome in varying numbers among individuals because of deletions, insertions, or duplications. These CNVs are common in apparently normal persons, but may also predispose toward or cause disease phenotypes (14). Advances in molecular genetic techniques now allow CNV analysis using a variety of microarray-based approaches including comparative genome hybridization (aCGH).

In recent years, SNP genotyping and CNV analysis have been utilized to identify gene mutations responsible for malformations of cortical development. Our laboratory is involved in ongoing efforts to uncover the genetic basis of disorders of cell proliferation, neuronal migration, and cortical organization, as well as other syndromes of neural development. Through national and international collaborations, our laboratory has identified and collected DNA samples from patients and families afflicted with diseases of neural development. Using both sporadic and familial cases, we have successfully employed array-based SNP and CNV approaches to uncover several disease-causing genetic mutations.

In Bayrakli et al. (15), our laboratory reported the case of a Turkish family in which 6 members were afflicted with autosomal recessive Parkinsonism. First, whole-genome linkage analysis was performed using a microarray system that contains 56,860 SNP

markers. The results of this initial genotyping demonstrated linkage to chromosome 6q26, the region housing the *parkin* gene (*PARK2*) (Figure 1). Mutations in *PARK2* have been shown to be associated with early-onset Parkinson's disease (16). Array-based comparative genome hybridization (aCGH) was then performed to determine the presence of copy number variations (CNVs) in the DNA of an affected patient relative to pooled human genomic DNA controls. The aCGH results revealed a homozygous microdeletion in the same region of chromosome 6q26 (Figure 2). PCR amplification within the predicted deleted region in 3 affected siblings and two unaffected relatives confirmed the presence of a homozygous microdeletion in exon 5 of the *PARK2* gene (Figure 3).

The Bayrakli et al. (15) study demonstrates the utility of molecular genetic techniques in identifying disease-causing gene mutations. Microarray-based SNP genotyping provided evidence of linkage to chromosome 6q26. Comparative genome hybridization or CNV analysis reaffirmed this locus as the region of interest and demonstrated a microdeletion in the parkin gene. Finally, PCR amplification confirmed the presence of a homozygous deletion in 3 affected siblings.

Molecular genetic techniques, including SNP genotyping and CNV analysis, have been utilized by several research groups, including ours, to investigate the gene mutations that underlie malformations of cortical development. These diseases and the genetic breakthroughs associated with them will be the focus of this manuscript.

Malformations of Cortical Development

Advances in molecular genetics have led to the elucidation of causative genes behind several human brain diseases. This has occurred concurrently with improved radiographic methods used to diagnose these disorders. Prior to 1980, malformations of cortical development (MCD) were studied by pathologists at autopsy. The advent of magnetic resonance imaging (MRI) allowed for earlier detection of these diseases. For the first time, phenotypic descriptions could be matched to radiologic findings. Interest in MCD has grown since then as the disorders have become increasingly recognized as significant causes of epilepsy, developmental delay, and other neurologic ailments.

Several proposed classification schemes have attempted to organize MCD based on our growing understanding of brain development. In 1996, Barkovich et al. (17) published a classification system that divided neural developmental pathology into disorders of cell proliferation, neuronal migration, or cortical organization. These 3 events—proliferation, migration, and organization—define embryonic cortical development. In the initial phase, neurons and glial cells proliferate in the ventricular and subventricular zones, respectively. Following the start of proliferation, postmitotic neurons migrate to the cortical plate. Finally, within the cortex, neurons undergo a process of vertical and horizontal organization as well as elaboration of their axonal and dendritic branches (18, 19).

MCD can result from abnormalities in any of the 3 stages of cortical development. In the initial classification (17), if a disease process involved more than one of the 3 stages, then it was classified based on the first abnormal step. Additionally, the classification separated *diffuse* and *focal* malformations because they were thought to have separate pathophysiology. The classification was revised in 2001 (20) and then again in 2005 (21) (Figure 1). In their most recent effort, the authors hoped to account for the rapid accumulation of new information regarding the genetic basis of many diseases of neural development. While the latest classification retains the 3 major groups of disorders described previously, it incorporates new information on the gene mutations that cause diseases of neural development (Figure 2).

The increased focus on the genetic basis of MCD allows for less reliance on the phenotypic characteristics of these disorders. A gene-oriented classification is necessary because mutations in different genes may result in the same phenotype, while various mutations in one gene may result in different phenotypes (21). Many of the genetic breakthroughs on MCD have occurred recently using novel molecular genetic approaches (Figure 2). These approaches have been utilized by several research groups, including ours, in order to uncover the genetic basis of disorders of cell proliferation, neuronal migration, and cortical organization, as well as the malformations of cortical development that are not otherwise classified.

Disorders of Cell Proliferation

Diseases in this group may be due to abnormal proliferation or apoptosis, resulting in an increase or decrease in the number of neurons or glial cells, or both (20). When the proliferation or apoptosis is diffuse, it leads to an abnormality in brain size, otherwise known as microcephaly or macrocephaly. Three main types of microcephalies occur: microcephaly with normal to thin cortex, extreme microcephaly with thick cortex (microlissencephaly), or microcephaly with extreme polymicrogyria (21). On the other hand, localized proliferation causes abnormal cell growth without a change in brain size. This set of disorders includes cortical hamartomas of tuberous sclerosis; cortical dysplasia associated with epilepsy; hemimegalencephaly (enlargement of one hemisphere leading to mental retardation and epilepsy); and neoplasms such as ganglioglioma, gangliocytoma, or dysembryoplastic neuroepithelial tumor.

Recent studies have identified several gene mutations associated with disorders of cell proliferation. Several genes have been shown to cause autosomal recessive microcephaly, including MCPH1 on chromosome 8p23 (22), ASPM on 1q31 (23, 24), CDK5RAP2 on 9q34 (25), CENPJ on 13q12.2 (25), and SLC25A19 on 17q25.3 (26). The ATR gene on 3q22-24 has been found to cause Seckel syndrome or microlissencephaly with short stature (24), while *TSC1* (27, 28) and *TSC2* (29, 30) on 9q32 and 16p13.3 were shown to cause cortical hamartomas of tuberous sclerosis.

These findings illustrate that various gene mutations may lead to similar phenotypes. Such investigations contribute significantly to our understanding of disorders of cell proliferation. Our laboratory has collected 13 familial or sporadic cases of disorders in this category including cortical dysplasia, microcephaly, and dysembryoplastic neuroepithelial tumor (DNET), as well as syndromes like infantile neuroaxonal dystrophy (INAD). We collected two familial cases of INAD and our genetic studies revealed two novel mutations in the *PLA2G6* gene, previously shown to be mutated in INAD. These results will be discussed at length in this manuscript.

Disorders of Neuronal Migration

These diseases, resulting from abnormal migration of neurons from the ventricular zone to the cerebral cortex, often present on MRI as gray matter in the subependymal or subcortical regions (20). Malformations within this group include lissencephaly, cobblestone complex, and heterotopia (21). Lissencephaly or "smooth brain" is characterized by a lack of gyri, abnormally thick cortex, and enlarged ventricles. Subcortical band heterotopia (SBH) consists of a subcortical band of gray matter separated from the cortex by a band of white matter. Both diseases comprise the so-called agyria-pachygyria-band spectrum. Cobblestone complex refers to a "cobblestone" cortex, abnormal white matter, large ventricles, and small brainstem and cerebellum (20). It is associated with congenital muscular dystrophy syndromes (37). Finally, heterotopia have various forms, ranging from periventricular to subcortical to marginal glioneuronal.

Periventricular nodular heterotopia consist of small masses of gray matter that line the ventricular walls and protrude into the lumen (38). Subcortical heterotopia (other than band heterotopia, described above) are less common than periventricular heterotopia. Depending on their size and location, subcortical heterotopia may result in developmental delay or mental retardation, hemiplegia, or epilepsy (20).

Several genes have been implicated in disorders of neuronal migration. Several groups have published gene mutations that underlie lissencephaly and subcortical band heterotopia, including the *DCX* gene on Xq22.3-23 (39-41), *ARX* on Xp22.13 (42, 43), *LIS1* on 17p13.3 (44-46), *RELN* on 7q22 (47). Mutations in the LARGE gene on 22q12.3-13.1 (48), POMT1 on 9q34.1 (49), FKRP on 19q13.3 (50, 51), and FCMD on 9q31 (52) have been shown to cause various syndromes within the cobblestone complex, while ARFGEF2 on 20q13.3 (53) and *FLNA* on Xq28 (54) are believed to mutated in bilateral periventricular nodular heterotopia.

In this category, our laboratory has collected 42 cases of disorders, including heterotopia, periventricular development anomalies, and lissencephaly, as well as syndromes like hereditary spastic paraplegia (HSP). For this latter syndrome, we have uncovered novel genetic findings based on a familial case of HSP. Specifically, we were able to demonstrate linkage of our kindred to the SPG11 locus on chromosome 15q. While SPG11 has been reported previously to be associated with cases of HSP, our results confirm and narrow the locus.

Disorders of Cortical Organization

Diseases in this category occur when neurons reach the cortex, but fail to form normal cortical layers or connections. They typically have abnormal gyri with normal cortical thickness (20). Common disorders include polymicrogyria (many small gyri separated by shallow sulci), schizencephaly (polymicrogyria with clefts), cortical dysplasia *without* balloon cells, and microdysgenesis (21). As with other MCD, these diseases typically present with developmental delay, cognitive deficits, and epilepsy.

Much work remains to be done on the genetic basis of the disorders of cortical organization. The only significant gene mutation identified has been that of *GPR56* on 16q13 in bilateral frontoparietal polymicrogyria (67). Our laboratory has collected 55 cases of disorders in this category that includes cortical developmental anomalies, polymicrogyria, and schizencephaly. These cases will allow us to shed us light on the genetic variations that cause disorders of cortical organization. Recently, we published the case of a patient with a disorder of cortical organization, Greig cephalopolysyndactyly (GCPS), and cerebral cavernous malformations (CCM). Our genetic studies uncovered a microdeletion in chromosome 7p, which resulted in the loss of the *GLI3* and *CCM2* genes. While deletions in these two genes have been previously shown to cause GCPS and CCM respectively, this is the first case in the literature of a patient with deletions in both genes and the hallmarks of both diseases. To our knowledge, the combination of GCPS and CCM represents a novel genetic syndrome, one that will be discussed further in this manuscript.

Malformations of Cortical Development, Not Otherwise Classified

This fourth category includes disorders that cannot be easily placed into the 3 aforementioned groups, including metabolic disorders, peroxisomal disorders, and unclassified syndromes. We have collected 65 patients with various syndromes of neural development, ranging from autism to childhood epilepsy.

STATEMENT OF PURPOSE & SPECIFIC AIMS

The purpose of this study is to utilize molecular genetic techniques, specifically SNP genotyping and CNV analysis, in order to find genetic mutations that cause diseases of neural development. This manuscript details our studies on three diseases in particular: INAD, HSP, and GCPS. Our aim is to uncover the gene mutations that cause these disorders so that we may develop a better understanding of the pathophysiology of these diseases specifically and malformations of neural development generally.

METHODS

Patient Identification and Collection of Blood Samples

The author of this manuscript attained approval for this study from the Yale Human Investigations Committee (Protocol 7680). The patients afflicted with MCD were identified by physicians at Yale New Haven Hospital as well as collaborators at other institutions in the United States and Europe. For patients identified at Yale New Haven Hospital, the author attained consent and collected their blood samples. For patient identified elsewhere, consent was attained and blood samples were collected by the collaborating physicians.

Isolation of Genomic DNA

Total genomic DNA was isolated from lymphocyte nuclei using a procedure described by Bell et al. (75). Ten milliliters of blood collected in a heparinized tube and then kept at 4°C was mixed with 90 ml of 0.32 M sucrose / 10 mM TrisHCl (pH 7.5) / 5 mM $MgCl^2$ / 1% Triton X-100 at 4°C to lyse all cells. The nuclei were collected by centrifugation at 1000 X g for 10 min. The nuclear pellet was suspended in 4.5 ml of 0.075 M NaCl / 0.024 M EDTA (pH 8.0) with a Pasteur pipette. Then 0.5 ml of 5% sodium dodecyl

sulfate and proteinase K at 2 mg/ml were added and the mixture was incubated for approximately 12 hr at 37°C.

The digest was gently mixed with 5 ml of phenol saturated with 20 mM Tris HCl (pH 8.0). Five milliliters of chloroform / isoamyl alcohol (24:1, vol/vol) was added and gentle mixing was continued. The phases were separated by centrifugation for 15 min at 1000 X g. The upper, aqueous, phase was removed and gently extracted with the chloroform / isoamyl alcohol mixture. After centrifugation, the aqueous phase was removed; 0.5 ml of 3 M sodium acetate and 11 ml of 100% ethanol (at room temperature) were added. The DNA was precipitated by inverting the tube several times and then removed with a Pasteur pipette and placed in 1 ml of 10 mM Tris HCl (pH 7.5) / 1 mM EDTA. The DNA was allowed to dissolve at 4°C. From 10 ml of blood, 20-50 μg of DNA was obtained. In cases where the yield is low, we incubate the DNA at -20°C in the presence of ammonium acetate. Genomic DNA was isolated by the author and laboratory technicians.

Single Nucleotide Polymorphism Genotyping

Genotyping was performed using the GeneChip Mapping 50K XbaI Array (Affymetrix Inc., Santa Clara, CA) containing 56,860 single nucleotide polymorphism (SNP) markers for genome-wide linkage analysis, according to the company's protocols. Briefly, after DNA was digested with XbaI, adapters were ligated to the product. Primers were then

used to amplify the product by PCR. Following purification, fragmentation, and labeling, biotin-labeled DNA product was hybridized to the Array chip. Arrays were then washed, stained, and scanned (76). Affymetrix Micro-Array Suite 5.0 software was utilized to obtain raw microarray feature intensities, the results of which were processed to derive SNP genotypes using the Affymetrix Genotyping Tools software package. SNP genotyping was performed by laboratory technicians.

Genechip Data Analysis

The Genome Analysis programs provided by Affymetrix were used for basic analysis of the Genechip data. Multipoint linkage analysis was performed using a UNIX-based program (Chunky). This program, initially described by Nahed et al. (76), parses the data into individual files that convey chromosome number, SNP markers, map distances, genotype calls, and allele frequencies. Final linkage analysis was then performed using Allegro software (DeCode Genetics, Inc) (77). We assumed an autosomal recessive inheritance pattern and assigned a 70% to 99% penetrance and a phenocopy rate of 0.001. Allele frequencies for the GeneChip SNPs were obtained from Affymetrix. Genechip analysis was performed by the author and by laboratory personnel.

Confirmation of Linkage Using Microsatellite Short Tandem Repeat Markers

Microsatellite short tandem repeat (STR) markers are used in order to fine map the linkage interval. Genomic regions with LOD scores approaching the theoretical maximum were further characterized and verified using STR markers within said regions according to the physical map data from the University of California at Santa Cruz (UCSC) Genome Browser (http://genome.ucsc.edu/index.html?org=Human). All available members of the family, both affected and unaffected, were genotyped. This strategy is often referred to as a 2-stage design in linkage analysis (78). All genotyping for microsatellite analysis was performed using PCR, with detection of fluorescent products on an ABI 3700 sequencer equipped with the Genescan and Genotyper software (ABI, Norwalk, CT). The author was involved in choosing the STR markers utilized in the confirmation of linkage. The PCR was performed by laboratory personnel.

Candidate Gene Mutational Analysis

Exon-intron boundaries of the candidate genes SPATA5L1 and SEMA6D within the linked interval were determined based on the University of California at Santa Cruz (UCSC) Genome Browser (NCBI Build 36.1). PCR primers were designed using PRIMER3 (http://frodo.wi.mit.edu/cgi-bin/primer3/primer3_www.cgi). Exon amplicons were amplified and sequenced using standard techniques. Mutational analysis was performed by the author and by laboratory personnel.

Array CGH for Copy Number Variant Analysis

Isolated DNA from the patients was submitted for whole genome and chromosome-specific aCGH analysis by high-resolution, tiled microarray (NimbleGen Systems, Madison, WI) to determine copy number variations (CNVs). These arrays employ 385,000 probes spanning all non-repetitive regions of the human genome on a single chip, tiling the full genome at a median probe spacing of 6,000 bp. The chromosome-specific arrays contain 385,000 oligomeric probes of lengths between 45–85mers with a median probe spacing of 10 bp. Patient DNA was cohybridized with pooled control DNA to determine copy number differences (deletions or amplifications) across the entire genome. Array CGH was performed by laboratory personnel.

Array CGH Data Analysis

All arrays were scanned with a GenePix 4000B Scanner (Molecular Devices Corporation, Sunnyvale, California) and normalized using QSPLINE (79) within the NimbleScan software package (Nimblegen Inc., Madison, WI). The normalized intensities were subsequently analyzed with the Circular Binary Segmentation (CBS) algorithm (80) to determine the significant breakpoints in log2 intensities along the chromosomes. Using average window sizes of 1X, 5X, 10X, and 20X (X=the median inter-probe distance), we determined the possible segments of the genome that were different between our patients and pooled, population-matched control samples. A segment (y) was considered to be significant if $y > 0.3$ or $y < -0.3$.

The normalized intensities were also analyzed with our Seed algorithm (Mason et al., in preparation), which creates windowed 5-probe averages along the genome after removing outlier data points (Dixon test) to detect additional small CNVs occasionally missed by CBS. Two patients with large-scale, known duplications in their genome were used to empirically determine a threshold for the Seed algorithm that kept sensitivity above 90% and specificity above 99.99%. We considered segment (y) to be significant in Seed if $y > 0.22$ or $y < -0.22$. Array CGH data analysis was performed by the author and by laboratory personnel.

Quantitative RT-PCR

Array CGH analysis results were confirmed with quantitative RT-PCR using the standard curve method for absolute quantitation. Primers were designed using Primer Express Software, version 2.0 (Applied Biosystems), with the following criteria: amplicon size of 80 to 200/250 bp, GC content of 20 to 80%, no more than two guanines or cytosines in the primer 3' end, and melting temperature (Tm) of 59 to 60°C. Finally, the Basic Local Alignment Search Tool (http://www.ncbi.nlm.nih.gov/blast/) was used for these primers.

The experimental design and calculations were performed as described by Applied Biosystems (User Bulletin #2). To determine copy number changes, fourfold ranges of five different serial dilutions from five pooled normal control DNA samples were used.

In addition, we used 5 ng of genomic DNA from the patient's DNA and pooled normal control DNA. The RT-PCRs were performed in triplicate for each reaction. The 15-µl reactions contained 1X final concentration of Power SYBR Green PCR Master Mix (part number 4367660, Applied Biosystems) and 400 nM of each primer (Invitrogen). Each experiment was performed using a 384-well optical PCR plate and the Applied Biosystems machine (model 7900HT) with default cycling conditions.

A standard curve was created using the calculated threshold cycle of each dilution for each gene. Amplifications were performed on the same diluted samples using primers for the reference and target genes. For all experimental samples, the target quantity was determined from the standard curve and divided by the target quantity of the normal reference DNA. To assess reaction specificity and to verify product identity, melting curve analysis was performed following amplification. We used the standard curves with an efficiency between 90% and 100%, which corresponds to a slope between 23.58 and 23.20. Quantitative PCR was performed by laboratory personnel.

RESULTS

Malformations of Cortical Development

Patient Collection

Our laboratory has collected 175 cases of malformations of cortical development (MCD), including 13 cases of disorders of cell proliferation, 42 cases of disorders of neuronal migration, 55 cases of disorders of cortical organization, and 65 cases of MCD not otherwise classified (Figure 4).

CNV Analysis

We are currently in the process of performing chip analysis on our samples (results not shown) in order to find the rate of homozygous deletions, heterozygous deletions, and amplifications relative to controls.

Disorders of Cell Proliferation

As stated earlier, our laboratory has collected 13 cases of disorders in this category, including 3 cases of cortical dysplasia, 1 case of microcephaly, 8 cases of

dysembryoplastic neuroepithelial tumor (DNET) as well as one familial case of infantile neuroaxonal dystrophy (presented below).

Infantile Neuroaxonal Dystrophy

Background

Infantile neuroaxonal dystrophy (INAD) is an autosomal recessive neurodegenerative disorder characterized by progressive motor and mental deterioration beginning in the first or second year of life. Clinically, the disease includes bilateral pyramidal tract signs, truncal hypotonia, and late-course spastic tetraplegia, blindness, and dementia (31). Death usually occurs before the age of 10 years.

While the pathophysiology of INAD has not been definitively elucidated, it is believed that defects in axonal transport (32) or synaptic transmission (33) lead to the histologic findings of axonal swelling and "spheroid bodies" in the central and peripheral nervous system.

MRI scanning of INAD patients has occasionally revealed iron accumulation in the globus pallidus, leading some to hypothesize that a disturbance in iron protein function plays an important role in the pathogenesis of this disease (34).

Recently, two studies have implicated mutations in *PLA2G6*, a gene encoding calcium-independent phospholipase A2, as being associated with INAD. In the first study, Morgan et al. identified 44 unique mutations in *PLA2G6* in patients affected with INAD and neurodegeneration with brain iron accumulation (NBIA) (35). In the second study, Khateeb et al. reported the identification of a unique *PLA2G6* mutation associated with INAD in two Israeli Bedouin families (36). Our laboratory collected two Turkish kindreds with INAD and found two novel mutations in *PLA2G6*.

Phenotype Assignment

Our laboratory collected two sporadic cases of INAD (Figure 5). In the first case, the affected children, DY, presented at the age of 2 years old with complaints of loss of ability to walk or speak and with foot abnormalities. DY also displayed signs of truncal hypotonia, manifested by an inability to sit up straight without support. DY was delivered at term in a normal spontaneous vaginal delivery. At six months, she was able to crawl and sit without support. She was normal until the age of 2 years, when she began deteriorating. At 3 years old, skin biopsy was performed, revealing distended demyelinated nerves around sweat glands and blood vessels. The axons contained granular, electron-dense material with occasional clefts, a histopathological finding consistent with infantile neuroaxonal dystrophy. This patient's sibling also had INAD and died at the age of 7 years. Neither parent is affected with the disease, consistent with an autosomal recessive trait.

The second affected child, MM, presented at the age of 1.5 years with complaints of losing ability to walk or speak. By the age of 1 year, the patient had been able to walk and speak words. A few months later, the patient presented with deterioration of both faculties. Skin biopsy revealed findings of distended axons with granular, electron dense material, consistent with INAD. No other members of this family have been affected with INAD.

The MRI scans on both patients showed no evidence of hypointensity in the globus pallidus, indicating a lack of iron accumulation. Both scans demonstrated signs of cerebellar atrophy on T2 weighted MRI as well a mild periventricular hyperintensity on Flair imaging.

DNA Sequencing

Direct *PLA2G6* sequencing using the DNA of the two affected children revealed two novel mutations in exons 12 and 15 of the gene. Both mutations were single nucleotide substitutions. In exon 12, an A → G mutation resulted in a substitution of arginine with glycine. In exon 15, a C → T mutation resulted in a substitution of threonine with methionine.

Disorders of Neuronal Migration

Our laboratory has collected 42 familial and sporadic cases of disorders in this category. These include 5 cases of heterotopia, 3 cases of periventricular developmental anomalies, 24 cases of lissencephaly, and a familial case of hereditary spastic paraplegia (presented below).

Hereditary Spastic Paraparesis

Background

Hereditary spastic paraplegias (HSP), also known as familial spastic paraparesis (FSP), are a genetically and clinically heterogeneous group of neurological disorders characterized by progressive lower extremity spasticity. HSPs can be associated with other neurological sequelae including neuropathy, retinopathy, dementia, icthyosis, mental retardation, deafness and seizures ("complicated" form), or by upper motor neuron findings including lower-extremity spasticity and neurogenic bladder alone ("uncomplicated" form). The diagnosis is confirmed through neurological testing, muscle biopsy, EMG, MRI, and detailed genetic history. The majority of HSP familial forms reported to date, up to 80%, demonstrate autosomal dominant patterns of expression, while the remainder demonstrate autosomal recessive and X-linked recessive inheritance patterns (55-57).

The first association of HSP with mental retardation and epilepsy, designated "SPERM" (OMIM 182610), was reported as a novel genetic disorder with an autosomal dominant pattern of inheritance (58). The family described was excluded from 8 previously described autosomal dominant HSP loci by linkage (59). Other families with complicated forms of HSP have been reported including an autosomal recessive form with a relatively constant clinical presentation of pyramidal tract signs in the lower extremities which progress to the upper extremities, gradual cognitive impairment, an onset before age 20, and radiographic findings of thinning of the corpus callosum (CC) and cortical atrophy known as HSP-TCC, or SPG11 (OMIM 604360) (60-66). Our laboratory is preparing a manuscript describing a new family from Eastern Turkey with autosomal recessive HSP associated with early-onset mental retardation, epilepsy and a variably thinned corpus callosum on MRI demonstrating linkage to the SPG11 locus at 15q13-15 using both SNP genotyping and CNV analysis. This data, when added to those previously reported, supports the notion that SPG11 is a phenotypically and genetically heterogeneous disorder.

Phenotype Assessment

The family was identified in Southeastern Turkey after the index case, a product of a consanguineous marriage, presented to medical attention with spastic paraparesis, mental retardation, and epilepsy. Clinical testing included magnetic resonance imaging (MRI), electromyography (EMG), electroencephalogram (EEG), cerebrospinal fluid analysis,

and other specific laboratory examinations such as routine blood work, blood thyroid hormone, ammonium, lactate levels, urine analysis.

Parents of the affected children were normal and consanguineous, providing evidence for an autosomal recessive inheritance pattern. Affected status was assigned after clinical documentation of prominent lower followed by upper extremity paraparesis with long (pyramidal) tract signs (spasticity, hyperreflexia, and bilateral Babinski sign), and epileptic discharges on electroencephalogram (EEG) (Figure 8).

Case 1 (V-1)

The index case was a four year-old female, a product of a consanguineous marriage, who presented with neurological decline. The patient was neurologically normal until the age of 6 months when parents became concerned with the child's lack of interactivity. By the age of 9 months, the child developed seizures which were controlled medically. On neurologic examination, the patient demonstrated motor and mental retardation, spasticity in the lower limbs, hyperreflexia, and an inability to sit without support. An MRI revealed a thinned corpus callosum on coronal T2 and sagittal T1 imaging (Figure 9).

Case 2 (V-2)

The second affected was the brother of the index case, a twelve year-old male. The patient developed normally but, as with Case 1, began having seizures at 10 months of

age. He also suffered from mental retardation, spasticity in lower and upper limbs, aphasia, hyperreflexia, and an inability to sit without support (imaging unavailable).

Case 3(V-3)

The third affected individual was a first cousin of the index case, also a product of a consanguineous marriage. This ten-year-old boy presented with seizures and mental retardation at age 6 months. He had difficulty swallowing solid food. Neurological examination revealed mental retardation, spasticity in the lower limbs, hyperreflexia, and inability to sit without support. MRI revealed mild, diffuse atrophy of grey and white matter with a thinned corpus callosum (Figure 9).

In all 3 patients, EEG studies showed myoclonic generalized epileptic discharges. Laboratory values provided no evidence for a lysosomal, mitochondrial, or peroxisomal disorder or a disturbance of amino acid or organic acid metabolism. CSF analysis was unremarkable.

Single Nucleotide Polymorphism Genotyping

We performed array-based genotyping on all available affected individuals and their parents (n=7). The 50K SNP arrays provide estimated information with a mean marker distance of 26 kb with an average of 53,970 genotypes scored per subject (SNP call-rates ranged between 92%–97%). Multipoint linkage analysis demonstrated a mean LOD

score of > 3 (maximum: 3.6287) within a 9.8 cM region between markers rs10518676 and rs2129773 on chromosome 15q15-q21 (Figures 10 and 11).

Linkage Using Microsatellite Short Tandem Repeat Markers

The linkage interval was verified and confirmed using seven highly polymorphic di and tetranucleotide microsatellite repeats across our linkage interval. As expected, the parents were heterozygous for the affected haplotype while the children with the HSP-TCC phenotype were homozygous for the affected haplotype (Figure 8).

Mutation screen

Screening of the candidate genes within the linkage interval, SPATA5L1 and SEMA6D failed to reveal any polymorphisms that segregated with the phenotype (data not shown).

Array CGH for Copy Number Analysis

Whole genome aCGH and chromosome 15-specific aCGH identified several copy number variations throughout the genome. None of these variations, however, were within the linkage interval and none segregated with the disease (Figure 12).

Disorders of Cortical Organization

Our laboratory has collected 55 familial and sporadic cases of these disorders, including 20 cortical developmental anomalies, 19 cases of polymicrogyria, 8 cases of schizencephaly, and one case of Greig cephalopolysyndactyly and cerebral cavernous malformations (presented below).

Greig Cephalopolysyndactyly and Cerebral Cavernous Malformation

Background

Greig cephalopolysyndactyly (GCPS) is a syndrome characterized by polydactyly, macrocephaly, and hypertelorism. Patients with severe GCPS can also present with mental retardation, seizures, and hydrocephalus. Mutations in *GLI3* at the chromosome 7p14 locus have been shown to cause GCPS (68).

Cerebral cavernous malformations (CCM) are abnormally dilated vascular channels, lined by a single layer of endothelium, that are prone to leakage resulting in cerebral hemorrhage. When symptomatic, the clinical manifestations can include headache, seizure, and neurological deficits. The heritability of CCM has been well established, and both familial and sporadic forms have been described. To date, three genes when mutated have been shown to cause CCM: *CCM1* on chromosome 7q21 (KRIT1) (69), *CCM2* on 7p13 (Malcavernin) (70, 71), and *CCM3* on 3q26 (PDCD10) (72, 73).

Our group reported the case of a patient who presented with a novel syndrome combining the clinical hallmarks of CCM and GCPS (74). High resolution CNV analysis, or comparative genome hybridization (aCGH), was used to identify the causal deletion on chromosome 7p that resulted in the heterozygous loss of both the *GLI3* and *CCM2* transcripts.

Phenotype Assessment

This 32-month-old girl presented to Yale University with a history of developmental delay. The mother's pregnancy and delivery were uncomplicated, and the child was born vaginally at a gestational age of 40 weeks (APGAR scores: 8 at 1 minute and 9 at 5 minutes). The family had no history of mental retardation, infant deaths, or multiple spontaneous abortions. The patient has two older siblings who were noted to be developmentally normal and without medical problems.

On examination the patient exhibited hypotonia with dysmorphic facial features, bilateral polysyndactyly of the great toes (Figure 6), proptosis of the left eye, and a wide-based stance. Her height and weight were in the 25th percentile, whereas her head circumference was in the 90th percentile. She had a prominent forehead, synophrys, mild thoracolumbar kyphosis, and a noncommunicating sacral dimple. Her neurological examination was nonfocal.

The facial features, hypotonia, and developmental delay indicated the possibility of a genetic syndrome involving polydactyly. To rule out chromosomal abnormalities, G-banded karyotyping was performed and was found to be normal (46, XX). The x-ray film studies confirmed bilateral polydactyly and showed normal hands and a kyphotic spine (Figure 6).

At age 4, seizures developed and the patient underwent additional neurological examination and brain imaging, which revealed the presence of multiple CCMs. The child was referred to the Yale Neurovascular Center. Axial T1-weighted MR imaging demonstrated multiple CCMs in the periventricular region as well as the subcortical parietal and frontal lobes (Figure 6). On detailed examination, we noted mild gyral abnormalities consisting of possible asymmetry of the central sulci (Figure 6).

Array CGH for Copy Number Analysis

Given the current overlap in clinical features between CCM and GCPS, the known involvement of *GLI3* on chromosome 7p in the latter syndrome, the recent identification of causal deletions of *CCM2* in some patients with CCM (71), and a normal G-banded karyotype in this patient, we elected to utilize array CGH to search for CNVs leading to this clinical picture. Array CGH revealed no CNVs in the regions of *CCM1* or *CCM3* (Figure 7). However, a possible deletion was detected at the *CCM2* locus on chromosome 7p, consisting of 466 probes with an average log2 intensity of less than 20.5, which exceeded the cutoff for statistical significance of 20.3. The putative deletion

covered 3 M base pairs mapping from 41.9 to 45 million bp on the short arm of the chromosome.

Quantitative PCR

Quantitative PCR confirmed a heterozygous deletion encompassing the genes *CCM2* and *GLI3* (Figure 7) as well as several intervening genes, including *HECWI*, *CAMK2B*, and *NPCL1* (Table 4). The quantitative RT-PCR analysis also confirmed two normal copies of the genes centromeric (*IGFBP1*, *TBRG4*, *ADCY1*, and *IGFBP3*) and telomeric (*INHBA* and *CDC2L5*) to the affected interval.

DISCUSSION

The results of the three studies presented above demonstrate the utility of SNP genotyping and CNV analysis in uncovering the genetic basis of MCD. Specifically, three diseases are presented in this manuscript: infantile neuroaxonal dystrophy, Greig cephalopolysyndactyly, and hereditary spastic paraparesis.

In the familial case of infantile neuroaxonal dystrophy, our results are the third, after Morgan et al. and Khateeb et al., to implicate *PLA2G6* as being associated with the disorder. The two novel mutations presented in this study along with the mutations in Morgan et al. will prove useful clinically in the diagnosis of INAD, which currently relies on nonspecific histologic findings on invasive biopsy. A recent paper in *Seminars in Pediatric Neurology* stated that once INAD is suspected, DNA testing should be utilized to confirm the diagnosis (81). In the future, genetic testing for this disease may replace tissue biopsy, which can be avoided altogether except in cases where testing fails to demonstrate a *PLA2G6* mutation.

The affected individuals in the INAD study, unlike a number of the individuals in Morgan et al., did not have high iron concentrations in the basal ganglia. The possibility exists that these represent two distinct disease processes: INAD without brain iron and INAD with brain iron. Nevertheless, *PLA2G6* mutations have been shown, in this and in previous findings, to be associated with INAD regardless of brain iron concentration.

Calcium-independent phospholipase A2, the protein product of *PLA2G6*, is involved in cell membrane homeostatis, arachidonic acid release, and leukotriene / prostaglandin synthesis. It has been hypothesized that a loss of function mutation in *PLA2G6* and the subsequent defect in phospholipase A2 lead to excessive levels of membrane phosphatidylcholine, which may result in the axonal pathology observed in INAD (35). The specificity of this effect on the central and peripheral nervous systems raises the question of *PLA2G6* expression patterns. Currently, our laboratory is studying the expression of *PLA2G6* in order to shed light on this issue.

In the case of the patient with Greig cephalopolysyndactyly and cerebral cavernous malformations, our laboratory reported a seemingly new clinical syndrome resulting from a heterozygous deletion affecting chromosome 7p14-13. Our results illustrate the utility of high-resolution array CGH in the study of suspected genetic syndromes. We used this technique to investigate possible variations in the three established CCM loci (7p, 7q, and 3q). We found a statistically significant CNV on chromosome 7p, which was then confirmed on quantitative RT-PCR to be a deletion of the interval containing the genes *CCM2* (causing CCMs) and *GLI3* (causing GCPS).

Greig cephalopolysyndactyly syndrome is characterized by polydactyly, hypertelorism, developmental delay, syndactyly, and macrocephaly. Moreover, two additional syndromes with clinical features overlapping those of GCPS have been described. Acrocallosal syndrome, like GCPS, is characterized by polysyndactyly, macrocephaly,

and hypertelorism; however, patients with this syndrome also show dysgenesis of the corpus callosum (82) and tend to have more severe developmental delay than those with GCPS. Pallister–Hall syndrome shares with GCPS the key features of postaxial polydactyly and developmental delay but does not include hypertelorism or macrocephaly (68). The case reported by our laboratory is the first instance of GCPS associated with CCMs as part of a broader syndrome marked by a 7p14-13 deletion.

In addition to *CCM2* and *GLI3*, deletions on several other genes within the interval were confirmed on quantitative RT-PCR (Table 4). However, bioinformatic analysis of sequence conservation of the brain-expressed genes within this region identified only *GLI3* as having a strongly conserved element (83) or highly conserved element (84) across vertebrates. This result suggests that these other transcripts within this interval may not be under strong stabilizing selection. In conjunction with the absence of any additional clinical features beyond those attributable to CCM or GCPS in the affected patient, this analysis suggests that heterozygous deletions of these additional transcripts may be well tolerated.

In the report on this patient, we characterized a novel syndrome consisting of CCMs, polydactyly, developmental delay, and hypertelorism resulting from a 7p14-13 deletion including the genes *CCM2* and *GLI3*. Our identification of the causative submicroscopic deletion, which was not identified using standard genetic testing methods, suggests that high resolution chromosomal analysis and neuroimaging studies are indicated when evaluating syndromic patients with neurological problems.

This manuscript also presents a familial case of hereditary spastic paraparesis. In this investigation, a member of our laboratory identified a family from eastern Turkey with autosomal recessive HSP, epilepsy, mental retardation, and a thinned corpus callosum (TCC) on MRI demonstrating linkage to the SPG11 locus at 15q15.1-q21.3, a region between 38.1 - 51 Mb. The clinical criteria for HSP-TCC are defined as normal motor development followed by a slowly progressive spastic paraparesis, mental retardation, and a very thin corpus callosum on imaging (64-66). Other clinical signs that have been reported include extrapyramidal signs, hyperreflexia, dysphagia, dysarthria, amyotrophy, urinary incontinence, muscle atrophy, and peripheral neuropathy with cortical atrophy and white matter changes on imaging (60-63). The average age of onset has been reported to be in the second decade (60).

In HSP, significant phenotypic variability exists within affected members of families with respect to clinical signs and radiographic signs. For example, some affected patients demonstrate various degrees of thinning of the corpus callosum on MRI, thought to represent a progressive finding of neuronal loss (60, 62, 63, 66). The family reported here differs from those previously reported with respect to the uniformly early onset of disease (in the first year of life) including epileptic seizures and a mildly-thinned corpus callosum on MRI, further expanding the phenotype. Interestingly, no cases of epilepsy were reported in any of the families demonstrating linkage to SPG11. The only prior reported case of HSP with epilepsy was from the family with the so-called autosomal

dominant “SPERM” syndrome (58), though others have reported affected patients with seizures late in disease progression (85).

Linkage analysis of the SPG11 locus for HSP was first reported by Martinez Murillo et al. (65) in 7 families from Italy and North America, between markers D15S1007 and D15S1012 on chromosome 15q13-15, a region of approximately 6.9 cM corresponding to 5 Mb on chromosome 15 (Figure 13). This linkage region was subsequently expanded (64) to between markers D15S971 and D15S117, a region of 26.7 cM corresponding to 23 Mb in 10 Japanese families with HSP-TCC. Originally described in the Japanese population (85-87), there have been several reports in the literature of families with HSP-TCC from different ethnicities, with the majority of families appearing to originate from the Mediterranean region (60-63, 65). Genetic linkage results in many of these families have confirmed or narrowed the SPG11 locus (60, 62, 63, 66). A recently published paper by Olmez et al. (61) reported linkage in 4 Turkish families in a region between markers D15S968 and D15S132. The authors argue that their results narrow the centromeric end of the region and, in effect, exclude the region defined by Martinez Murillo et al. (65). Our linkage data confirm the results of Olmez et al. (61), also excluding the first reported interval (Figure 13).

Chromosomal copy number alterations can lead to over activation or inactivation of genes in humans leading to cancer or disease phenotypes. Comparative Genomic Hybridization (CGH) is a method to detect chromosomal copy number by comparing hybridization intensity of a patient’s DNA to a control DNA sample (88) and has become

an important tool in rapid identification of functional mutations within linkage intervals (89-91). In the case of a family with HSP, we hypothesized that CNVs within the linkage interval might be causative of the disease phenotype. We performed array-based whole-genome and chromosome 15-specific CGH in the family. Analysis of the array results did not show any CNV within the linkage interval in affected patients. Furthermore, mutational analysis of the potential candidate genes SPATA5L1 and SEMA6D in this region did not reveal any causative mutations (60, 63).

In addition to HSP, a second congenital neurological disorder demonstrates linkage to the same interval as SPG11. Amyotrophic lateral sclerosis type 5 (ALS5) is characterized by gait disturbance, spasticity, mental retardation, and severe bulbar and pseudobulbar findings and demonstrates linkage between markers D15S146 and D15S123 (92). It is possible that this phenotype is a part of the same spectrum of neurological disorders as HSP-TCC, caused by different mutations within the same gene (that ALS5 is an allelic disorder to HSP-TCC) supporting the idea that HSP-TCC represents a syndrome with broad phenotypic and genetic heterogeneity. This hypothesis is plausible as it was previously demonstrated that ALS2 is allelic to infantile ascending hereditary spastic paralysis (IAHSP) (93). More compelling is the fact that many families with autosomal recessive HSP-TCC (families with affected members fitting the clinical criteria of the syndrome) exclude by linkage the reported SPG11 locus (60, 62, 66). This clearly argues in favor of genetic heterogeneity of the disorder.

Our results for HSP confirm previously published linkage analysis in families demonstrating linkage to the SPG11 locus on 15q and demonstrate the absence of CNV within the linkage interval in this family. The phenotype reported here adds to the broad spectrum of clinical findings within the HSP-TCC syndrome. These results, when dovetailed with those previously published, demonstrate phenotypic heterogeneity of a common clinical entity with a common genetic cause. The explanation of phenotypic variation within patients linking to the SPG11 locus is likely multifactorial and a combination of non-genetic, compound genetic, and mutation-specific causes.

The three cases presented in this manuscript demonstrate the utility of molecular genetic approaches, particularly SNP genotyping and CNV analysis, in uncovering the genetic basis of neural developmental disease. In the familial case of INAD, our laboratory was able to find two novel mutations in the *PLA2G6* gene. In the sporadic case of GCPS and CCM, CNV analysis using aCGH was used to identify the chromosome 7 deletion affecting the *GLI3* and *CCM2* genes. These results establish this unique clinical presentation as a novel syndrome combining the hallmarks of GCPS and CCM. Finally, in the case of the Turkish family with HSP, high density SNP genotyping was used for whole genome linkage analysis, allowing us to further narrow the previously established linkage interval for this autosomal recessive disease. Although in this case we were not able to identify a causative gene mutation, narrowing the interval of the SPG11 locus on chromosome 15 will help guide future efforts to hunt the gene(s) responsible for HSP.

Our laboratory continues to perform mutational analysis on candidate genes in this locus as well as other regions associated with neurologic disorders. The molecular genetic approaches described in this manuscript will further enhance our understanding of the pathophysiology of diseases of neural development.

REFERENCES

1. Kruglyak, L., and Nickerson, D.A. 2001. Variation is the spice of life. *Nat Genet* 27:234-236.

2. 2003. The International HapMap Project. *Nature* 426:789-796.

3. Hirschhorn, J.N., and Daly, M.J. 2005. Genome-wide association studies for common diseases and complex traits. *Nat Rev Genet* 6:95-108.

4. Risch, N., and Merikangas, K. 1996. The future of genetic studies of complex human diseases. *Science* 273:1516-1517.

5. Syvanen, A.C. 2005. Toward genome-wide SNP genotyping. *Nat Genet* 37 Suppl:S5-10.

6. Schaid, D.J., Guenther, J.C., Christensen, G.B., Hebbring, S., Rosenow, C., Hilker, C.A., McDonnell, S.K., Cunningham, J.M., Slager, S.L., Blute, M.L., et al. 2004. Comparison of microsatellites versus single-nucleotide polymorphisms in a genome linkage screen for prostate cancer-susceptibility Loci. *Am J Hum Genet* 75:948-965.

7. John, S., Shephard, N., Liu, G., Zeggini, E., Cao, M., Chen, W., Vasavda, N., Mills, T., Barton, A., Hinks, A., et al. 2004. Whole-genome scan, in a complex disease, using 11,245 single-nucleotide polymorphisms: comparison with microsatellites. *Am J Hum Genet* 75:54-64.

8. Saba, T.G., Montpetit, A., Verner, A., Rioux, P., Hudson, T.J., Drouin, R., and Drouin, C.A. 2005. An atypical form of erythrokeratodermia variabilis maps to chromosome 7q22. *Hum Genet* 116:167-171.

9. Koed, K., Wiuf, C., Christensen, L.L., Wikman, F.P., Zieger, K., Moller, K., von der Maase, H., and Orntoft, T.F. 2005. High-density single nucleotide polymorphism array defines novel stage and location-dependent allelic imbalances in human bladder tumors. *Cancer Res* 65:34-45.

10. Sigurdsson, S., Nordmark, G., Goring, H.H., Lindroos, K., Wiman, A.C., Sturfelt, G., Jonsen, A., Rantapaa-Dahlqvist, S., Moller, B., Kere, J., et al. 2005. Polymorphisms in the tyrosine kinase 2 and interferon regulatory factor 5 genes are associated with systemic lupus erythematosus. *Am J Hum Genet* 76:528-537.

11. Hinds, D.A., Seymour, A.B., Durham, L.K., Banerjee, P., Ballinger, D.G., Milos, P.M., Cox, D.R., Thompson, J.F., and Frazer, K.A. 2004. Application of pooled genotyping to scan candidate regions for association with HDL cholesterol levels. *Hum Genomics* 1:421-434.

12. Pinkel, D., and Albertson, D.G. 2005. Array comparative genomic hybridization and its applications in cancer. *Nat Genet* 37 Suppl:S11-17.

13. Sebat, J., Lakshmi, B., Troge, J., Alexander, J., Young, J., Lundin, P., Maner, S., Massa, H., Walker, M., Chi, M., et al. 2004. Large-scale copy number polymorphism in the human genome. *Science* 305:525-528.

14. Redon, R., Ishikawa, S., Fitch, K.R., Feuk, L., Perry, G.H., Andrews, T.D., Fiegler, H., Shapero, M.H., Carson, A.R., Chen, W., et al. 2006. Global variation in copy number in the human genome. *Nature* 444:444-454.

15. Bayrakli, F., Bilguvar, K., Mason, C.E., DiLuna, M.L., Bayri, Y., Gungor, L., Terzi, M., Mane, S.M., Lifton, R.P., State, M.W., et al. 2007. Rapid identification of disease-causing mutations using copy number analysis within linkage intervals. *Hum Mutat* 28:1236-1240.

16. Lucking, C.B., Durr, A., Bonifati, V., Vaughan, J., De Michele, G., Gasser, T., Harhangi, B.S., Meco, G., Denefle, P., Wood, N.W., et al. 2000. Association between early-onset Parkinson's disease and mutations in the parkin gene. *N Engl J Med* 342:1560-1567.

17. Barkovich, A.J., Kuzniecky, R.I., Dobyns, W.B., Jackson, G.D., Becker, L.E., and Evrard, P. 1996. A classification scheme for malformations of cortical development. *Neuropediatrics* 27:59-63.

18. Barkovich, A.J., Gressens, P., and Evrard, P. 1992. Formation, maturation, and disorders of brain neocortex. *AJNR Am J Neuroradiol* 13:423-446.

19. Marin-Padilla, M. 1995. Prenatal development of fibrous (white matter), protoplasmic (gray matter), and layer I astrocytes in the human cerebral cortex: a Golgi study. *J Comp Neurol* 357:554-572.

20. Barkovich, A.J., Kuzniecky, R.I., Jackson, G.D., Guerrini, R., and Dobyns, W.B. 2001. Classification system for malformations of cortical development: update 2001. *Neurology* 57:2168-2178.

21. Barkovich, A.J., Kuzniecky, R.I., Jackson, G.D., Guerrini, R., and Dobyns, W.B. 2005. A developmental and genetic classification for malformations of cortical development. *Neurology* 65:1873-1887.

22. Jackson, A.P., Eastwood, H., Bell, S.M., Adu, J., Toomes, C., Carr, I.M., Roberts, E., Hampshire, D.J., Crow, Y.J., Mighell, A.J., et al. 2002. Identification of microcephalin, a protein implicated in determining the size of the human brain. *Am J Hum Genet* 71:136-142.

23. Bond, J., Roberts, E., Mochida, G.H., Hampshire, D.J., Scott, S., Askham, J.M., Springell, K., Mahadevan, M., Crow, Y.J., Markham, A.F., et al. 2002. ASPM is a major determinant of cerebral cortical size. *Nat Genet* 32:316-320.

24. Bond, J., Scott, S., Hampshire, D.J., Springell, K., Corry, P., Abramowicz, M.J., Mochida, G.H., Hennekam, R.C., Maher, E.R., Fryns, J.P., et al. 2003. Protein-truncating mutations in ASPM cause variable reduction in brain size. *Am J Hum Genet* 73:1170-1177.

25. Bond, J., Roberts, E., Springell, K., Lizarraga, S.B., Scott, S., Higgins, J., Hampshire, D.J., Morrison, E.E., Leal, G.F., Silva, E.O., et al. 2005. A centrosomal mechanism involving CDK5RAP2 and CENPJ controls brain size. *Nat Genet* 37:353-355.

26. Rosenberg, M.J., Agarwala, R., Bouffard, G., Davis, J., Fiermonte, G., Hilliard, M.S., Koch, T., Kalikin, L.M., Makalowska, I., Morton, D.H., et al. 2002. Mutant deoxynucleotide carrier is associated with congenital microcephaly. *Nat Genet* 32:175-179.

27. Haines, J.L., Short, M.P., Kwiatkowski, D.J., Jewell, A., Andermann, E., Bejjani, B., Yang, C.H., Gusella, J.F., and Amos, J.A. 1991. Localization of one gene for tuberous sclerosis within 9q32-9q34, and further evidence for heterogeneity. *Am J Hum Genet* 49:764-772.

28. Harris, R.M., Carter, N.P., Griffiths, B., Goudie, D., Hampson, R.M., Yates, J.R., Affara, N.A., and Ferguson-Smith, M.A. 1993. Physical mapping within the tuberous sclerosis linkage group in region 9q32-q34. *Genomics* 15:265-274.

29. 1993. Identification and characterization of the tuberous sclerosis gene on chromosome 16. *Cell* 75:1305-1315.

30. Kandt, R.S., Haines, J.L., Smith, M., Northrup, H., Gardner, R.J., Short, M.P., Dumars, K., Roach, E.S., Steingold, S., Wall, S., et al. 1992. Linkage of an important gene locus for tuberous sclerosis to a chromosome 16 marker for polycystic kidney disease. *Nat Genet* 2:37-41.

31. Aicardi, J., and Castelein, P. 1979. Infantile neuroaxonal dystrophy. *Brain* 102:727-748.

32. Wakai, S., Asanuma, H., Tachi, N., Ishikawa, Y., and Minami, R. 1993. Infantile neuroaxonal dystrophy: axonal changes in biopsied muscle tissue. *Pediatr Neurol* 9:309-311.

33. Walkley, S.U., Baker, H.J., Rattazzi, M.C., Haskins, M.E., and Wu, J.Y. 1991. Neuroaxonal dystrophy in neuronal storage disorders: evidence for major GABAergic neuron involvement. *J Neurol Sci* 104:1-8.

34. Gelman, B.B. 1995. Iron in CNS disease. *J Neuropathol Exp Neurol* 54:477-486.

35. Morgan, N.V., Westaway, S.K., Morton, J.E., Gregory, A., Gissen, P., Sonek, S., Cangul, H., Coryell, J., Canham, N., Nardocci, N., et al. 2006. PLA2G6, encoding a phospholipase A2, is mutated in neurodegenerative disorders with high brain iron. *Nat Genet* 38:752-754.

36. Khateeb, S., Flusser, H., Ofir, R., Shelef, I., Narkis, G., Vardi, G., Shorer, Z., Levy, R., Galil, A., Elbedour, K., et al. 2006. PLA2G6 mutation underlies infantile neuroaxonal dystrophy. *Am J Hum Genet* 79:942-948.

37. Dubowitz, V. 1994. 22nd ENMC sponsored workshop on congenital muscular dystrophy held in Baarn, The Netherlands, 14-16 May 1993. *Neuromuscul Disord* 4:75-81.

38. Barkovich, A.J., and Kjos, B.O. 1992. Gray matter heterotopias: MR characteristics and correlation with developmental and neurologic manifestations. *Radiology* 182:493-499.

39. des Portes, V., Francis, F., Pinard, J.M., Desguerre, I., Moutard, M.L., Snoeck, I., Meiners, L.C., Capron, F., Cusmai, R., Ricci, S., et al. 1998. doublecortin is the major gene causing X-linked subcortical laminar heterotopia (SCLH). *Hum Mol Genet* 7:1063-1070.

40. Gleeson, J.G., Allen, K.M., Fox, J.W., Lamperti, E.D., Berkovic, S., Scheffer, I., Cooper, E.C., Dobyns, W.B., Minnerath, S.R., Ross, M.E., et al. 1998. Doublecortin, a brain-specific gene mutated in human X-linked lissencephaly and double cortex syndrome, encodes a putative signaling protein. *Cell* 92:63-72.

41. Pilz, D.T., Matsumoto, N., Minnerath, S., Mills, P., Gleeson, J.G., Allen, K.M., Walsh, C.A., Barkovich, A.J., Dobyns, W.B., Ledbetter, D.H., et al. 1998. LIS1 and XLIS (DCX) mutations cause most classical lissencephaly, but different patterns of malformation. *Hum Mol Genet* 7:2029-2037.

42. Kato, M., Das, S., Petras, K., Kitamura, K., Morohashi, K., Abuelo, D.N., Barr, M., Bonneau, D., Brady, A.F., Carpenter, N.J., et al. 2004. Mutations of ARX are associated with striking pleiotropy and consistent genotype-phenotype correlation. *Hum Mutat* 23:147-159.

43. Kitamura, K., Yanazawa, M., Sugiyama, N., Miura, H., Iizuka-Kogo, A., Kusaka, M., Omichi, K., Suzuki, R., Kato-Fukui, Y., Kamiirisa, K., et al. 2002. Mutation of ARX causes abnormal development of forebrain and testes in mice and X-linked lissencephaly with abnormal genitalia in humans. *Nat Genet* 32:359-369.

44. Cardoso, C., Leventer, R.J., Matsumoto, N., Kuc, J.A., Ramocki, M.B., Mewborn, S.K., Dudlicek, L.L., May, L.F., Mills, P.L., Das, S., et al. 2000. The location and type of mutation predict malformation severity in isolated lissencephaly caused by abnormalities within the LIS1 gene. *Hum Mol Genet* 9:3019-3028.

45. Pilz, D.T., Kuc, J., Matsumoto, N., Bodurtha, J., Bernadi, B., Tassinari, C.A., Dobyns, W.B., and Ledbetter, D.H. 1999. Subcortical band heterotopia in rare affected males can be caused by missense mutations in DCX (XLIS) or LIS1. *Hum Mol Genet* 8:1757-1760.

46. Reiner, O., Carrozzo, R., Shen, Y., Wehnert, M., Faustinella, F., Dobyns, W.B., Caskey, C.T., and Ledbetter, D.H. 1993. Isolation of a Miller-Dieker lissencephaly gene containing G protein beta-subunit-like repeats. *Nature* 364:717-721.

47. Hong, S.E., Shugart, Y.Y., Huang, D.T., Shahwan, S.A., Grant, P.E., Hourihane, J.O., Martin, N.D., and Walsh, C.A. 2000. Autosomal recessive lissencephaly with cerebellar hypoplasia is associated with human RELN mutations. *Nat Genet* 26:93-96.

48. Longman, C., Brockington, M., Torelli, S., Jimenez-Mallebrera, C., Kennedy, C., Khalil, N., Feng, L., Saran, R.K., Voit, T., Merlini, L., et al. 2003. Mutations in the human LARGE gene cause MDC1D, a novel form of congenital muscular dystrophy with severe mental retardation and abnormal glycosylation of alpha-dystroglycan. *Hum Mol Genet* 12:2853-2861.

49. Beltran-Valero de Bernabe, D., Currier, S., Steinbrecher, A., Celli, J., van Beusekom, E., van der Zwaag, B., Kayserili, H., Merlini, L., Chitayat, D., Dobyns, W.B., et al. 2002. Mutations in the O-mannosyltransferase gene POMT1 give rise to the severe neuronal migration disorder Walker-Warburg syndrome. *Am J Hum Genet* 71:1033-1043.

50. Beltran-Valero de Bernabe, D., Voit, T., Longman, C., Steinbrecher, A., Straub, V., Yuva, Y., Herrmann, R., Sperner, J., Korenke, C., Diesen, C., et al. 2004. Mutations in the FKRP gene can cause muscle-eye-brain disease and Walker-Warburg syndrome. *J Med Genet* 41:e61.

51. Topaloglu, H., Brockington, M., Yuva, Y., Talim, B., Haliloglu, G., Blake, D., Torelli, S., Brown, S.C., and Muntoni, F. 2003. FKRP gene mutations cause congenital muscular dystrophy, mental retardation, and cerebellar cysts. *Neurology* 60:988-992.

52. de Bernabe, D.B., van Bokhoven, H., van Beusekom, E., Van den Akker, W., Kant, S., Dobyns, W.B., Cormand, B., Currier, S., Hamel, B., Talim, B., et al. 2003. A homozygous nonsense mutation in the fukutin gene causes a Walker-Warburg syndrome phenotype. *J Med Genet* 40:845-848.

53. Sheen, V.L., Ganesh, V.S., Topcu, M., Sebire, G., Bodell, A., Hill, R.S., Grant, P.E., Shugart, Y.Y., Imitola, J., Khoury, S.J., et al. 2004. Mutations in ARFGEF2 implicate vesicle trafficking in neural progenitor proliferation and migration in the human cerebral cortex. *Nat Genet* 36:69-76.

54. Fox, J.W., Lamperti, E.D., Eksioglu, Y.Z., Hong, S.E., Feng, Y., Graham, D.A., Scheffer, I.E., Dobyns, W.B., Hirsch, B.A., Radtke, R.A., et al. 1998. Mutations in filamin 1 prevent migration of cerebral cortical neurons in human periventricular heterotopia. *Neuron* 21:1315-1325.

55. Reid, E. 2003. Many pathways lead to hereditary spastic paraplegia. *Lancet Neurol* 2:210.

56. Fink, J.K. 2006. Hereditary spastic paraplegia. *Curr Neurol Neurosci Rep* 6:65-76.

57. Fink, J.K. 2003. The hereditary spastic paraplegias: nine genes and counting. *Arch Neurol* 60:1045-1049.

58. Gigli, G.L., Diomedi, M., Bernardi, G., Placidi, F., Marciani, M.G., Calia, E., Maschio, M.C., and Neri, G. 1993. Spastic paraplegia, epilepsy, and mental retardation in several members of a family: a novel genetic disorder. *Am J Med Genet* 45:711-716.

59. Lo Nigro, C., Cusano, R., Gigli, G.L., Forabosco, P., Valente, M., Ravazzolo, R., Diomedi, M., and Seri, M. 2003. Genetic heterogeneity in inherited spastic paraplegia associated with epilepsy. *Am J Med Genet A* 117:116-121.

60. Stevanin, G., Montagna, G., Azzedine, H., Valente, E.M., Durr, A., Scarano, V., Bouslam, N., Cassandrini, D., Denora, P.S., Criscuolo, C., et al. 2006. Spastic paraplegia with thin corpus callosum: description of 20 new families, refinement of the SPG11 locus, candidate gene analysis and evidence of genetic heterogeneity. *Neurogenetics* 7:149-156.

61. Olmez, A., Uyanik, G., Ozgul, R.K., Gross, C., Cirak, S., Elibol, B., Anlar, B., Winner, B., Hehr, U., Topaloglu, H., et al. 2006. Further clinical and genetic characterization of SPG11: hereditary spastic paraplegia with thin corpus callosum. *Neuropediatrics* 37:59-66.

62. Lossos, A., Stevanin, G., Meiner, V., Argov, Z., Bouslam, N., Newman, J.P., Gomori, J.M., Klebe, S., Lerer, I., Elleuch, N., et al. 2006. Hereditary spastic

paraplegia with thin corpus callosum: reduction of the SPG11 interval and evidence for further genetic heterogeneity. *Arch Neurol* 63:756-760.

63. Winner, B., Uyanik, G., Gross, C., Lange, M., Schulte-Mattler, W., Schuierer, G., Marienhagen, J., Hehr, U., and Winkler, J. 2004. Clinical progression and genetic analysis in hereditary spastic paraplegia with thin corpus callosum in spastic gait gene 11 (SPG11). *Arch Neurol* 61:117-121.

64. Shibasaki, Y., Tanaka, H., Iwabuchi, K., Kawasaki, S., Kondo, H., Uekawa, K., Ueda, M., Kamiya, T., Katayama, Y., Nakamura, A., et al. 2000. Linkage of autosomal recessive hereditary spastic paraplegia with mental impairment and thin corpus callosum to chromosome 15A13-15. *Ann Neurol* 48:108-112.

65. Martinez Murillo, F., Kobayashi, H., Pegoraro, E., Galluzzi, G., Creel, G., Mariani, C., Farina, E., Ricci, E., Alfonso, G., Pauli, R.M., et al. 1999. Genetic localization of a new locus for recessive familial spastic paraparesis to 15q13-15. *Neurology* 53:50-56.

66. Casali, C., Valente, E.M., Bertini, E., Montagna, G., Criscuolo, C., De Michele, G., Villanova, M., Damiano, M., Pierallini, A., Brancati, F., et al. 2004. Clinical and genetic studies in hereditary spastic paraplegia with thin corpus callosum. *Neurology* 62:262-268.

67. Piao, X., Hill, R.S., Bodell, A., Chang, B.S., Basel-Vanagaite, L., Straussberg, R., Dobyns, W.B., Qasrawi, B., Winter, R.M., Innes, A.M., et al. 2004. G protein-coupled receptor-dependent development of human frontal cortex. *Science* 303:2033-2036.

68. Johnston, J.J., Olivos-Glander, I., Killoran, C., Elson, E., Turner, J.T., Peters, K.F., Abbott, M.H., Aughton, D.J., Aylsworth, A.S., Bamshad, M.J., et al. 2005. Molecular and clinical analyses of Greig cephalopolysyndactyly and Pallister-Hall syndromes: robust phenotype prediction from the type and position of GLI3 mutations. *Am J Hum Genet* 76:609-622.

69. Laberge-le Couteulx, S., Jung, H.H., Labauge, P., Houtteville, J.P., Lescoat, C., Cecillon, M., Marechal, E., Joutel, A., Bach, J.F., and Tournier-Lasserve, E. 1999. Truncating mutations in CCM1, encoding KRIT1, cause hereditary cavernous angiomas. *Nat Genet* 23:189-193.

70. Denier, C., Goutagny, S., Labauge, P., Krivosic, V., Arnoult, M., Cousin, A., Benabid, A.L., Comoy, J., Frerebeau, P., Gilbert, B., et al. 2004. Mutations within the MGC4607 gene cause cerebral cavernous malformations. *Am J Hum Genet* 74:326-337.

71. Liquori, C.L., Berg, M.J., Siegel, A.M., Huang, E., Zawistowski, J.S., Stoffer, T., Verlaan, D., Balogun, F., Hughes, L., Leedom, T.P., et al. 2003. Mutations in a

gene encoding a novel protein containing a phosphotyrosine-binding domain cause type 2 cerebral cavernous malformations. *Am J Hum Genet* 73:1459-1464.

72. Bergametti, F., Denier, C., Labauge, P., Arnoult, M., Boetto, S., Clanet, M., Coubes, P., Echenne, B., Ibrahim, R., Irthum, B., et al. 2005. Mutations within the programmed cell death 10 gene cause cerebral cavernous malformations. *Am J Hum Genet* 76:42-51.

73. Guclu, B., Ozturk, A.K., Pricola, K.L., Bilguvar, K., Shin, D., O'Roak, B.J., and Gunel, M. 2005. Mutations in apoptosis-related gene, PDCD10, cause cerebral cavernous malformation 3. *Neurosurgery* 57:1008-1013.

74. Bilguvar, K., Bydon, M., Bayrakli, F., Ercan-Sencicek, A.G., Bayri, Y., Mason, C., DiLuna, M.L., Seashore, M., Bronen, R., Lifton, R.P., et al. 2007. A novel syndrome of cerebral cavernous malformation and Greig cephalopolysyndactyly. Laboratory investigation. *J Neurosurg* 107:495-499.

75. Bell, G.I., Karam, J.H., and Rutter, W.J. 1981. Polymorphic DNA region adjacent to the 5' end of the human insulin gene. *Proc Natl Acad Sci U S A* 78:5759-5763.

76. Nahed, B.V., Seker, A., Guclu, B., Ozturk, A.K., Finberg, K., Hawkins, A.A., DiLuna, M.L., State, M., Lifton, R.P., and Gunel, M. 2005. Mapping a Mendelian form of intracranial aneurysm to 1p34.3-p36.13. *Am J Hum Genet* 76:172-179.

77. Gudbjartsson, D.F., Jonasson, K., Frigge, M.L., and Kong, A. 2000. Allegro, a new computer program for multipoint linkage analysis. *Nat Genet* 25:12-13.

78. Elston, R.C., Guo, X., and Williams, L.V. 1996. Two-stage global search designs for linkage analysis using pairs of affected relatives. *Genet Epidemiol* 13:535-558.

79. Workman, C., Jensen, L.J., Jarmer, H., Berka, R., Gautier, L., Nielser, H.B., Saxild, H.H., Nielsen, C., Brunak, S., and Knudsen, S. 2002. A new non-linear normalization method for reducing variability in DNA microarray experiments. *Genome Biol* 3:research0048.

80. Olshen, A.B., Venkatraman, E.S., Lucito, R., and Wigler, M. 2004. Circular binary segmentation for the analysis of array-based DNA copy number data. *Biostatistics* 5:557-572.

81. Hayflick, S.J. 2006. Neurodegeneration with brain iron accumulation: from genes to pathogenesis. *Semin Pediatr Neurol* 13:182-185.

82. Johnston, J.J., Olivos-Glander, I., Turner, J., Aleck, K., Bird, L.M., Mehta, L., Schimke, R.N., Heilstedt, H., Spence, J.E., Blancato, J., et al. 2003. Clinical and molecular delineation of the Greig cephalopolysyndactyly contiguous gene

deletion syndrome and its distinction from acrocallosal syndrome. *Am J Med Genet A* 123:236-242.

83. Bejerano, G., Pheasant, M., Makunin, I., Stephen, S., Kent, W.J., Mattick, J.S., and Haussler, D. 2004. Ultraconserved elements in the human genome. *Science* 304:1321-1325.

84. Siepel, A., Bejerano, G., Pedersen, J.S., Hinrichs, A.S., Hou, M., Rosenbloom, K., Clawson, H., Spieth, J., Hillier, L.W., Richards, S., et al. 2005. Evolutionarily conserved elements in vertebrate, insect, worm, and yeast genomes. *Genome Res* 15:1034-1050.

85. Nakamura, A., Izumi, K., Umehara, F., Kuriyama, M., Hokezu, Y., Nakagawa, M., Shimmyozu, K., Izumo, S., and Osame, M. 1995. Familial spastic paraplegia with mental impairment and thin corpus callosum. *J Neurol Sci* 131:35-42.

86. Ueda, M., Katayama, Y., Kamiya, T., Mishina, M., Igarashi, H., Okubo, S., Senda, M., Iwabuchi, K., and Terashi, A. 1998. Hereditary spastic paraplegia with a thin corpus callosum and thalamic involvement in Japan. *Neurology* 51:1751-1754.

87. Iwabuchi, K., Kubota, Y., Hanihara, T., and Nagatomo, H. 1994. [Three patients of complicated form of autosomal recessive hereditary spastic paraplegia associated with hypoplasia of the corpus callosum]. *No To Shinkei* 46:941-947.

88. Kallioniemi, A., Kallioniemi, O.P., Sudar, D., Rutovitz, D., Gray, J.W., Waldman, F., and Pinkel, D. 1992. Comparative genomic hybridization for molecular cytogenetic analysis of solid tumors. *Science* 258:818-821.

89. Pinkel, D., Segraves, R., Sudar, D., Clark, S., Poole, I., Kowbel, D., Collins, C., Kuo, W.L., Chen, C., Zhai, Y., et al. 1998. High resolution analysis of DNA copy number variation using comparative genomic hybridization to microarrays. *Nat Genet* 20:207-211.

90. Pollack, J.R., Perou, C.M., Alizadeh, A.A., Eisen, M.B., Pergamenschikov, A., Williams, C.F., Jeffrey, S.S., Botstein, D., and Brown, P.O. 1999. Genome-wide analysis of DNA copy-number changes using cDNA microarrays. *Nat Genet* 23:41-46.

91. Solinas-Toldo, S., Lampel, S., Stilgenbauer, S., Nickolenko, J., Benner, A., Dohner, H., Cremer, T., and Lichter, P. 1997. Matrix-based comparative genomic hybridization: biochips to screen for genomic imbalances. *Genes Chromosomes Cancer* 20:399-407.

92. Hentati, A., Ouahchi, K., Pericak-Vance, M.A., Nijhawan, D., Ahmad, A., Yang, Y., Rimmler, J., Hung, W., Schlotter, B., Ahmed, A., et al. 1998. Linkage of a

commoner form of recessive amyotrophic lateral sclerosis to chromosome 15q15-q22 markers. *Neurogenetics* 2:55-60.

93. Eymard-Pierre, E., Lesca, G., Dollet, S., Santorelli, F.M., di Capua, M., Bertini, E., and Boespflug-Tanguy, O. 2002. Infantile-onset ascending hereditary spastic paralysis is associated with mutations in the alsin gene. *Am J Hum Genet* 71:518-527.

FIGURES

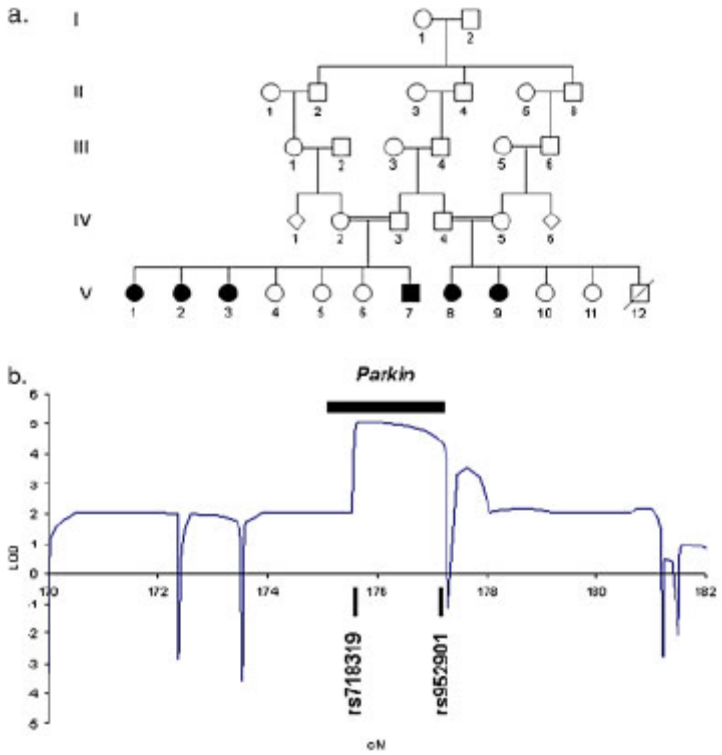

Figure 1: Parkinsonian family pedigree and linkage. a: Family pedigree (colored shapes designate family members with Parkinsonism). b: Linkage analysis using SNP microarrays demonstrates linkage with a LOD score of 5.08 (LOD > 3 represents significance) to a region of chromosome 6 housing the *parkin* gene. Adapted from Bayrakli et al. (15).

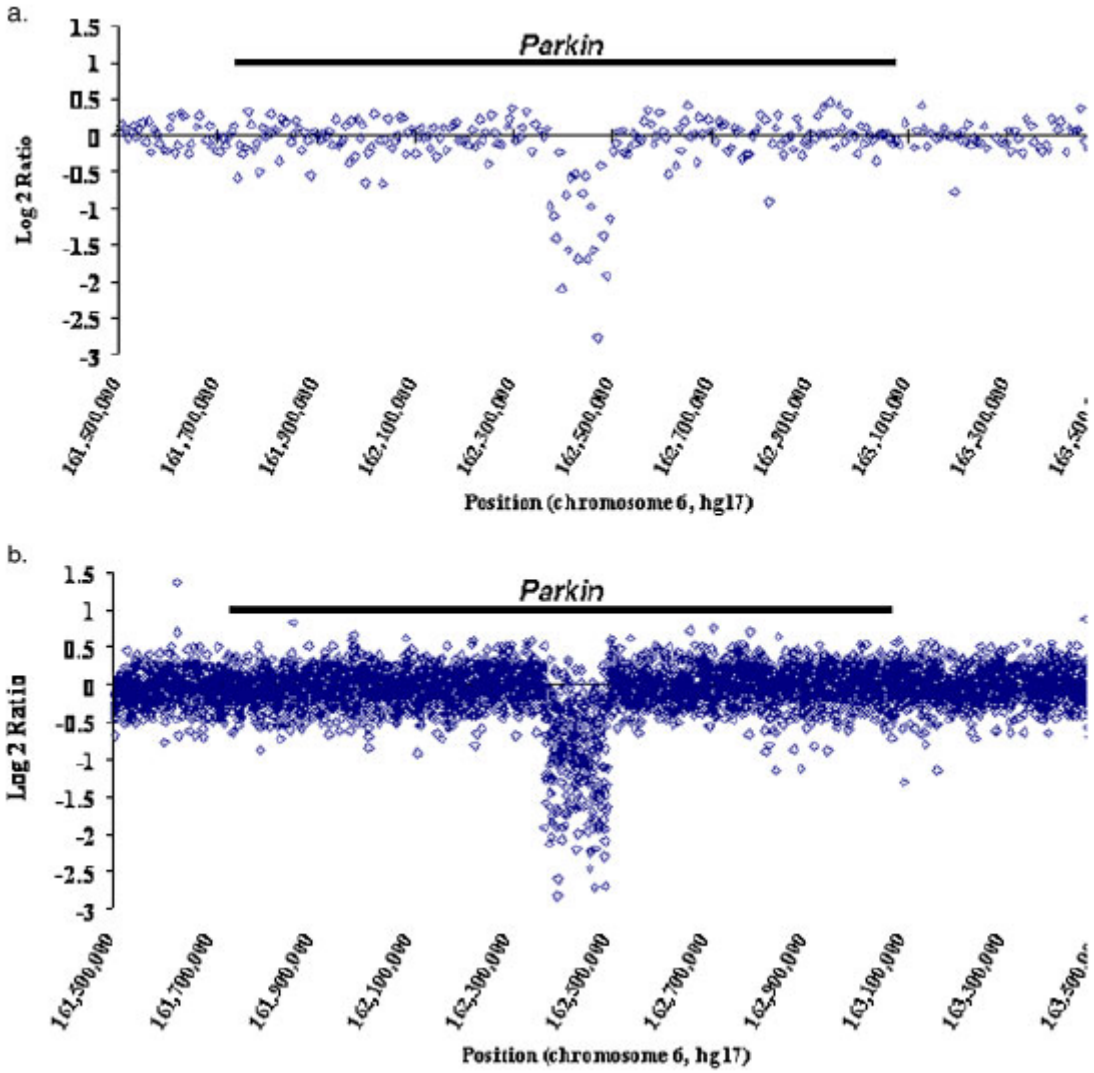

Figure 2: Parkinsonian family copy number analysis. a: Scatter plot of whole genome array-based comparative genome hybridization demonstrates a region within the linkage interval predicting a homozygous microdeletion. Scattered points represent normalized log2 ratios (y) for probes along the chromosome. A segment was considered to be significant if $y > 0.3$ or $y < -0.3$. These results show a region with an average log2 ratio (y) of -1.16, suggesting a homozygous deletion. b: Scatter plot of aCGH specific for chromosome 6 demonstrates a higher density of probes and prediction of homozygous microdeletion. The black bar represents the *parkin* gene. Adapted from Bayrakli et al. (15).

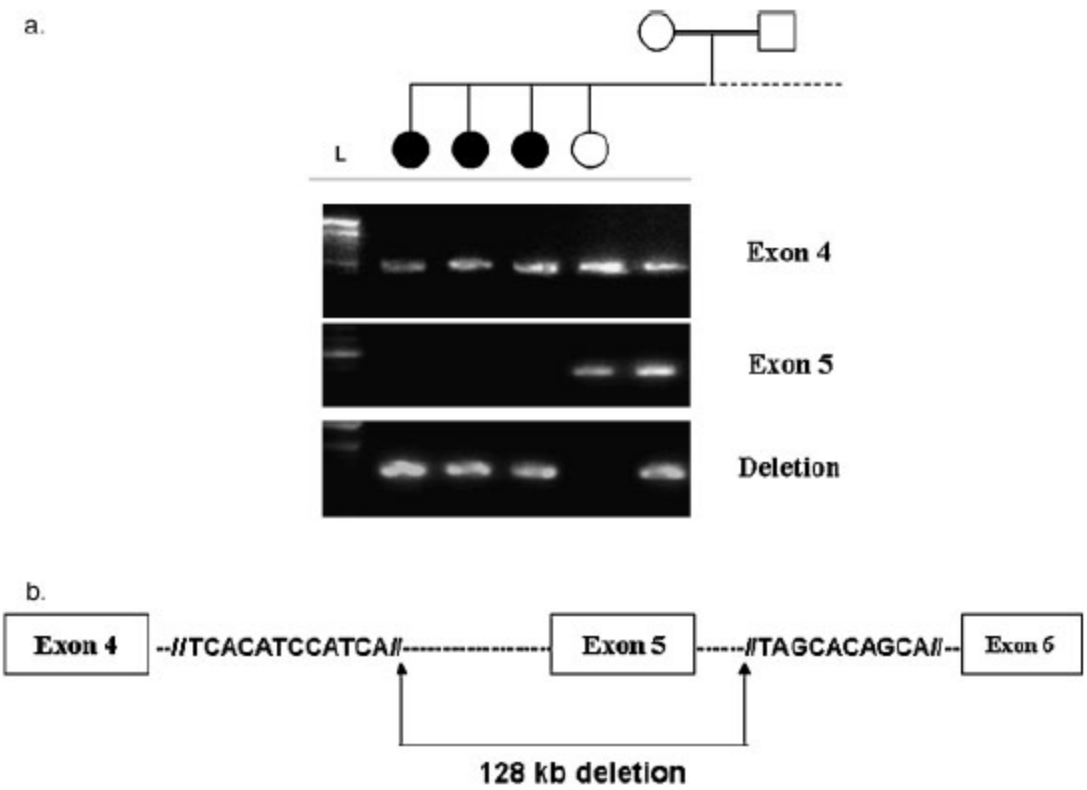

Figure 3: Parkinsonian family PCR deletion. a: PCR confirmation of the microdeletion. The top image represents amplification using intronic primers immediately flanking exon 4, confirming the presence of this exon in all family members. The middle image demonstrates amplification using primers that flank exon 5, showing a microdeletion in 3 affected siblings. b: This diagram illustrates the location of the microdeletion in the *parkin* gene. Adapted from Bayrakli et al. (15).

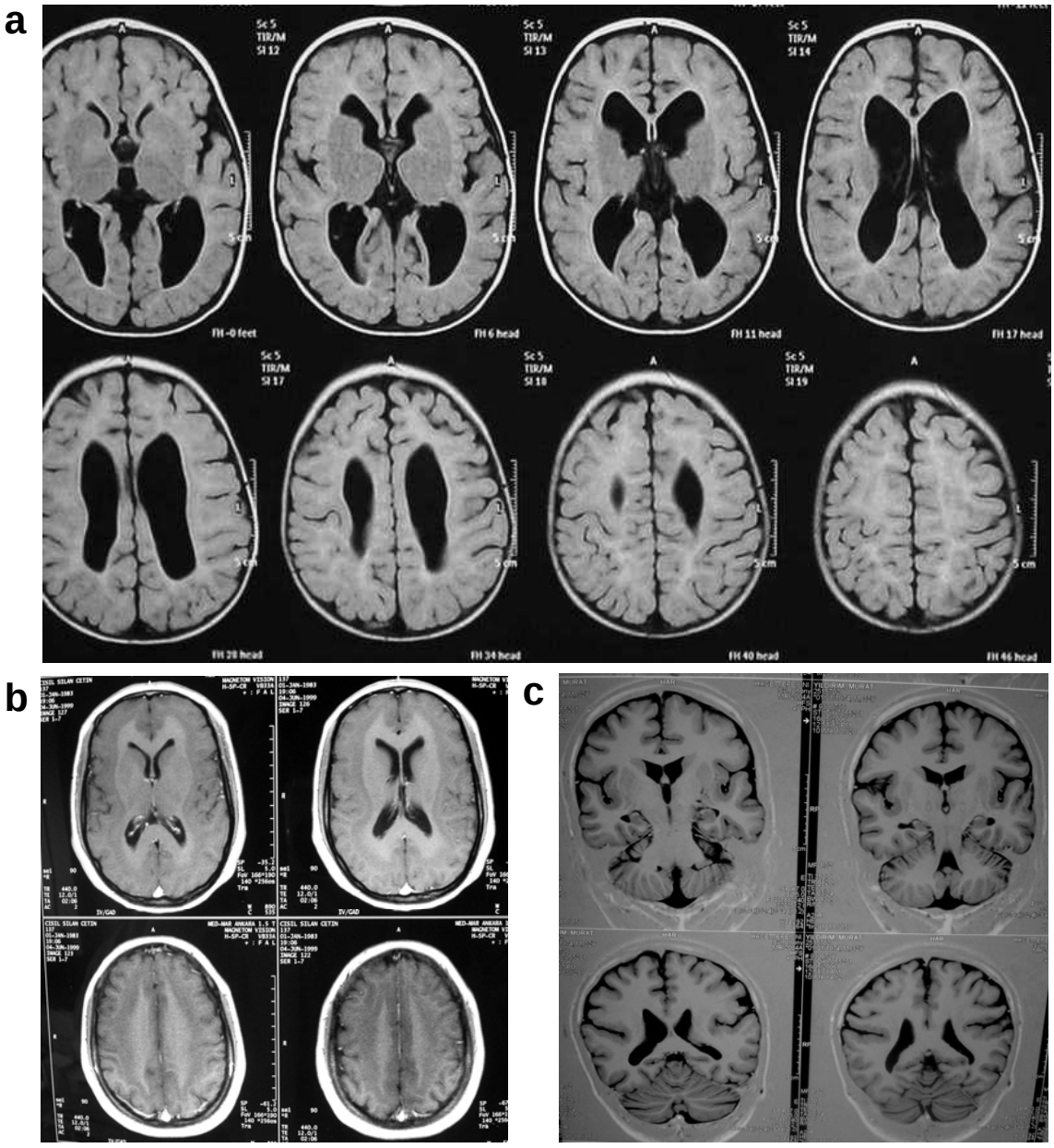

Figure 4: Images of malformations of cortical development. The diseases presented in these image include corpus callosum hyperplasia, a disorder of cell proliferation (a); subcortical band heterotopia or "double cortex," a disorder of neuronal migration (b); and polymicrogyria, a disorder of cortical organization (c).

INAD-I

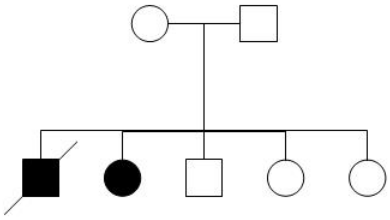

INAD-II

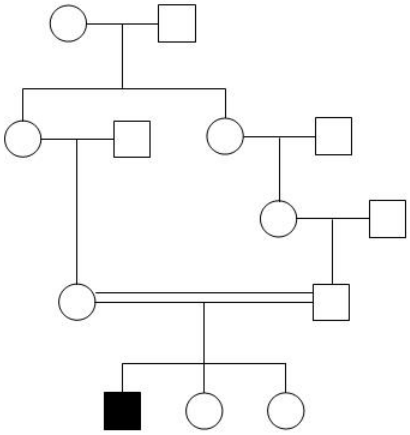

Figure 5: Two sporadic cases of INAD. In the first kindred, the dark circle represents a young child affected with INAD. Her brother, who was also had INAD, has passed (dark square with line). In the second kindred, a young child, the offspring of a consanguineous marriage, is also affected with INAD.

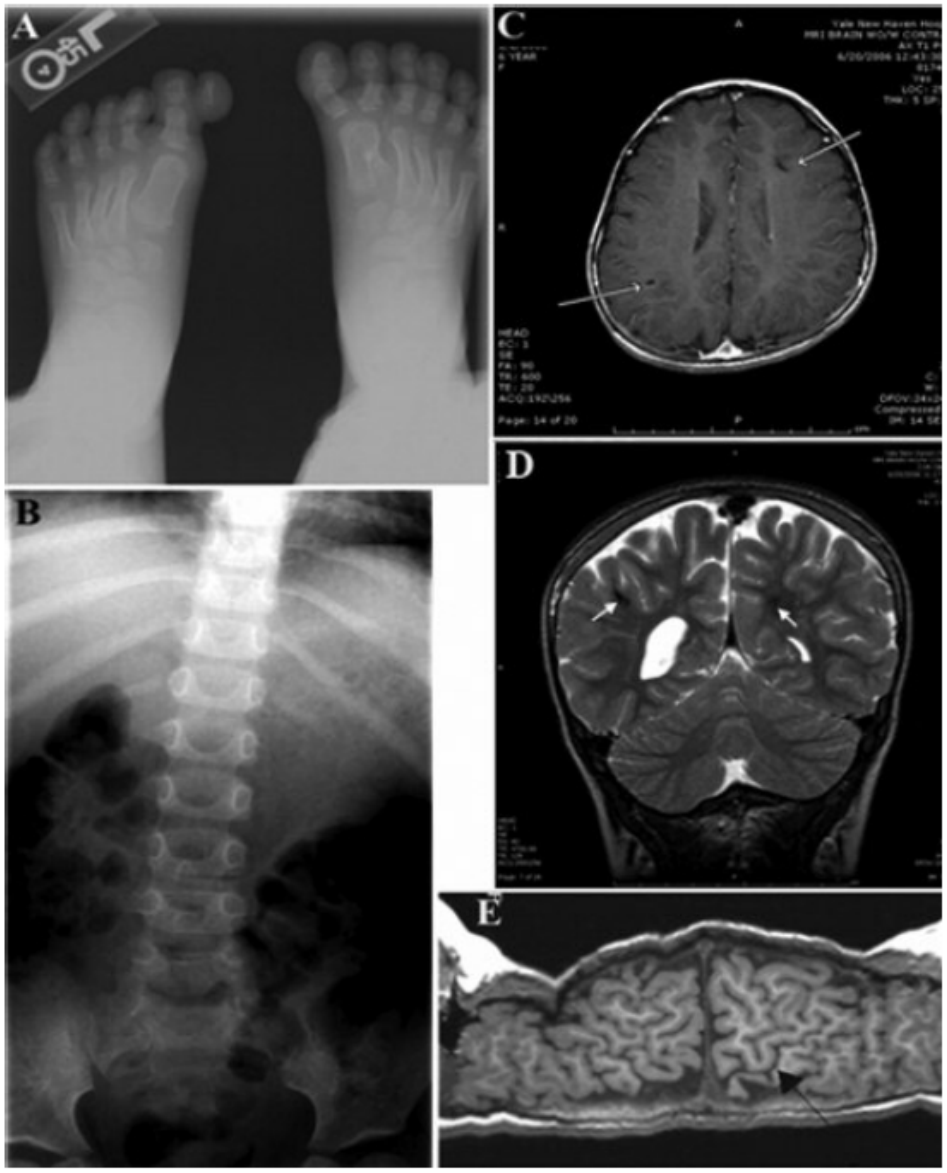

Figure 6: GCPS patient imaging. Radiographs obtained in a 32-month old girl, demonstrating bilateral polysyndactyly of the great toes (a) and scoliosis of the spine (b). Serial axial T1 (c) and T2-weighted (d) MR images obtained in the patient at 4 years of age, revealing subcortical CCMs (arrows) in the right parietal and left frontal lobes as well as a left periventricular CCM. Reformatted MR image (e) showing a normal central sulcus on the left side (arrow) and an asymmetrically formed central sulcus on the right. Adapted from Bilguvar et al. (74).

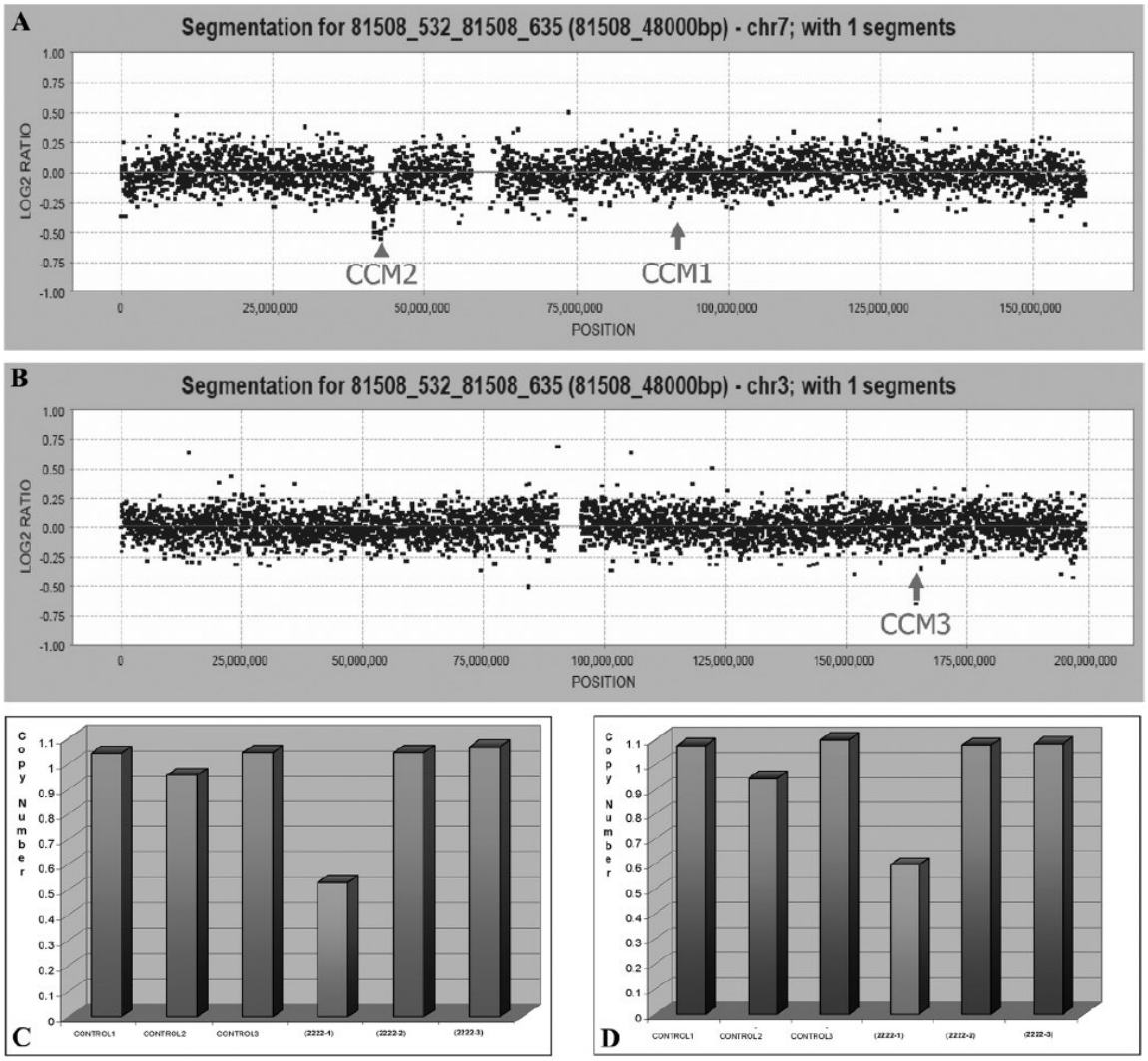

Figure 7: GCPS patient CNV and QPCR results. Graphs depicting the results of CNV analysis. On chromosome 7, a deletion was revealed within the CCM2 locus (a, arrowhead), but no apparent CNVs within the CCM1 locus (a, arrow). With this analysis, gene deletions are represented by negative log2 ratios of the signal intensity relative to normal. To be significant, the log2 ratio (y axis) must be less than 20.3. The log2 ratio at the CCM2 region is less than 20.5, indicating the presence of a deletion in that locus. There is no CNV within the CCM3 locus (b). Bar graphs of quantitative RT-PCR of CCM2 (c) and GLI3 (d) showing approximately half of the relative amplification of each respective gene amplicon, consistent with the presence of a heterozygous deletion in the affected patient (2222-1) within the CNV interval. The controls and parents (father 2222-2 and mother 2222-3) demonstrate full amplification of each respective gene amplicon. Adapted from Bilguvar et al. (74).

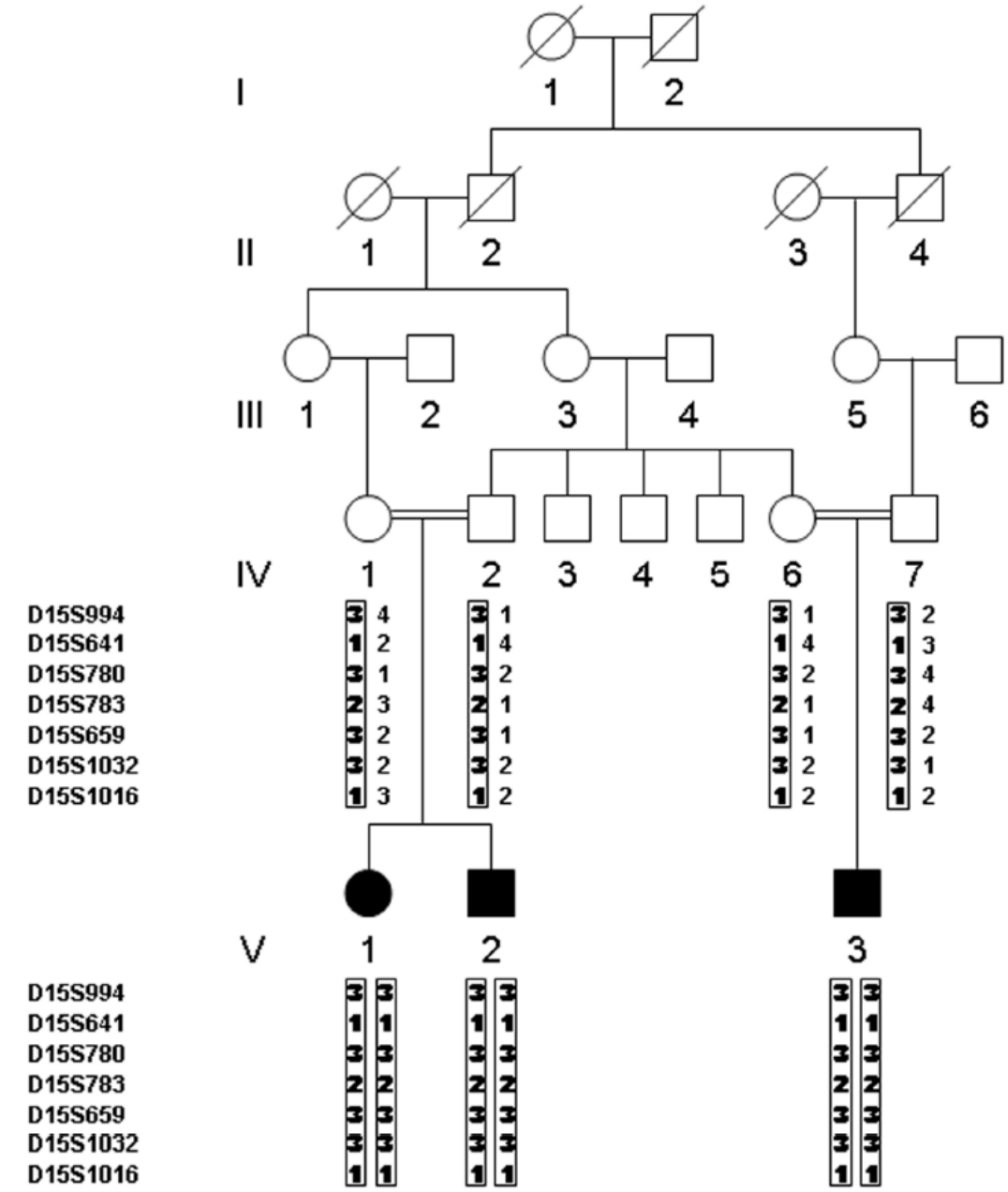

Figure 8: HSP family pedigree with STS marker haplotypes. Filled symbols show affected individuals, males are represented with square symbols, females with circles. The pattern, given the consanguinity, suggests autosomal recessive inheritance. Below affected family members V1-3 and their respective parents note the haplotype as determined by STS marker genotyping between markers D15S994 and D15S1016.

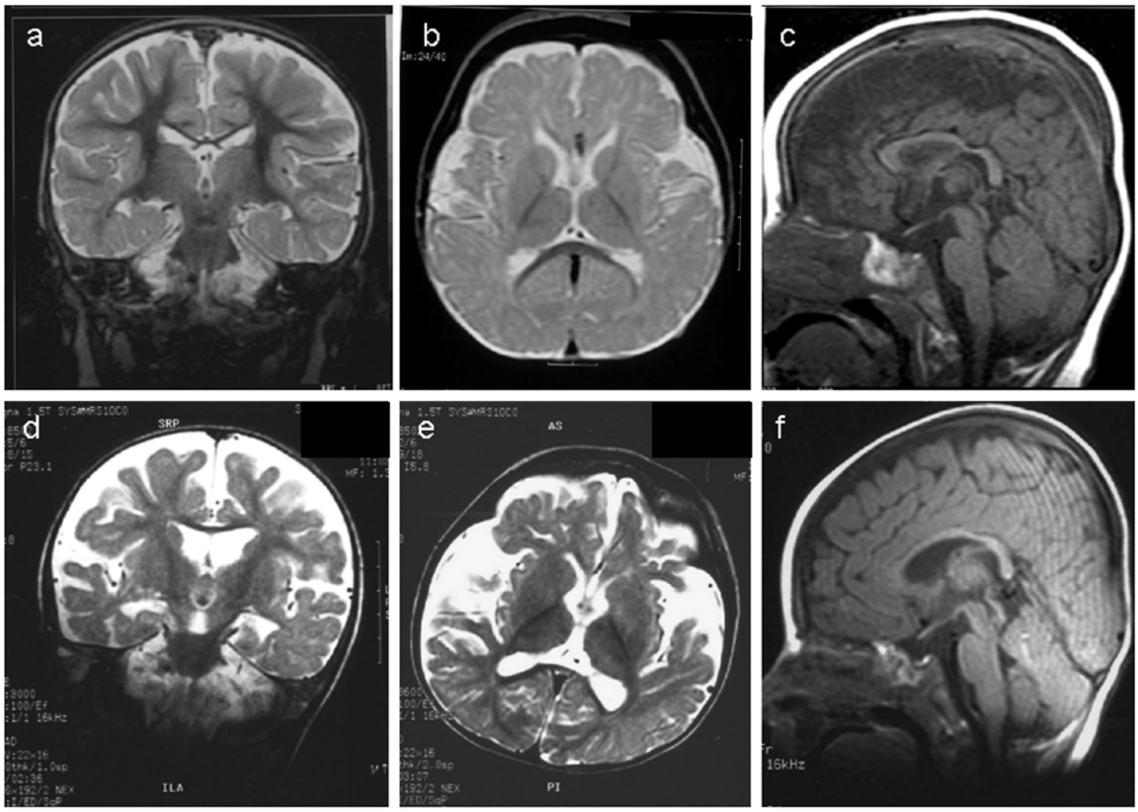

Figure 9: HSP cases V1 (a-c) and V3 (d-f) imaging. Patient V1 coronal (a) and axial (b) T2-weighted MRI images through the thalamus and 3rd ventricle demonstrate diffuse enlargement of the subarachnoid spaces along the convexities likely due to gray and white matter loss. Midline sagittal (c) T1-weighted MRI demonstrates the thinned corpus callosum. The cerebellum, pons, and medulla appear normal. Patient V3 coronal (d) and axial (e) T2-weighted MRI images through the thalamus and 3rd ventricle again demonstrate diffuse enlargement of the subarachnoid spaces along the convexities likely due to gray and white matter loss. Midline sagittal (f) T1-weighted MRI similarly demonstrates the thinned corpus callosum.

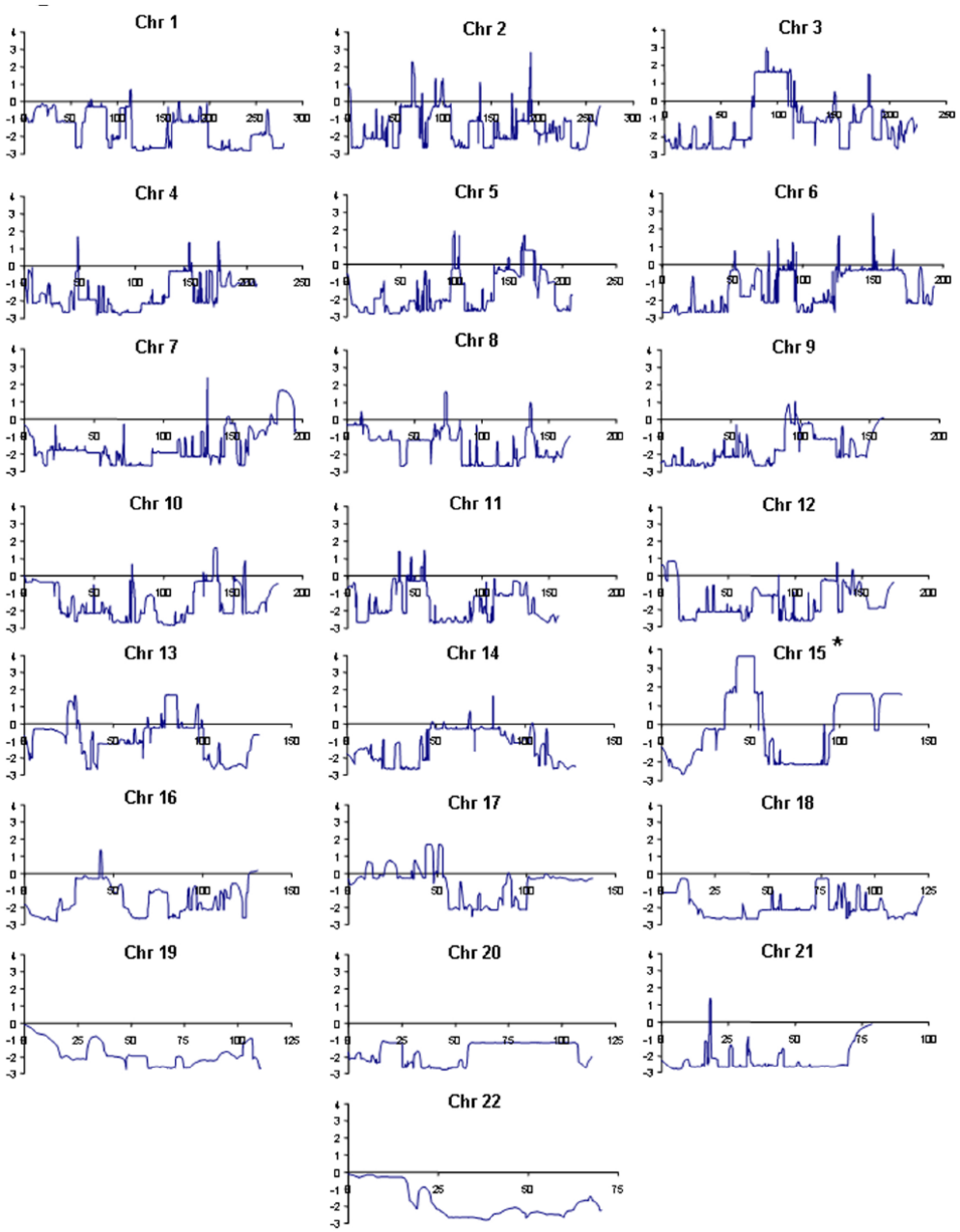

Figure 10: HSP family array-based SNP genotyping results. Genotyping results using the GeneChip Mapping 50K XbaI Array. Figure demonstrates multipoint linkage analysis plots for each chromosome. X axis = cM distance along the chromosome. Y axis = LOD score. Results are plotted after analysis using Chunky followed by the Allegro software. * denotes chromosome 15 results.

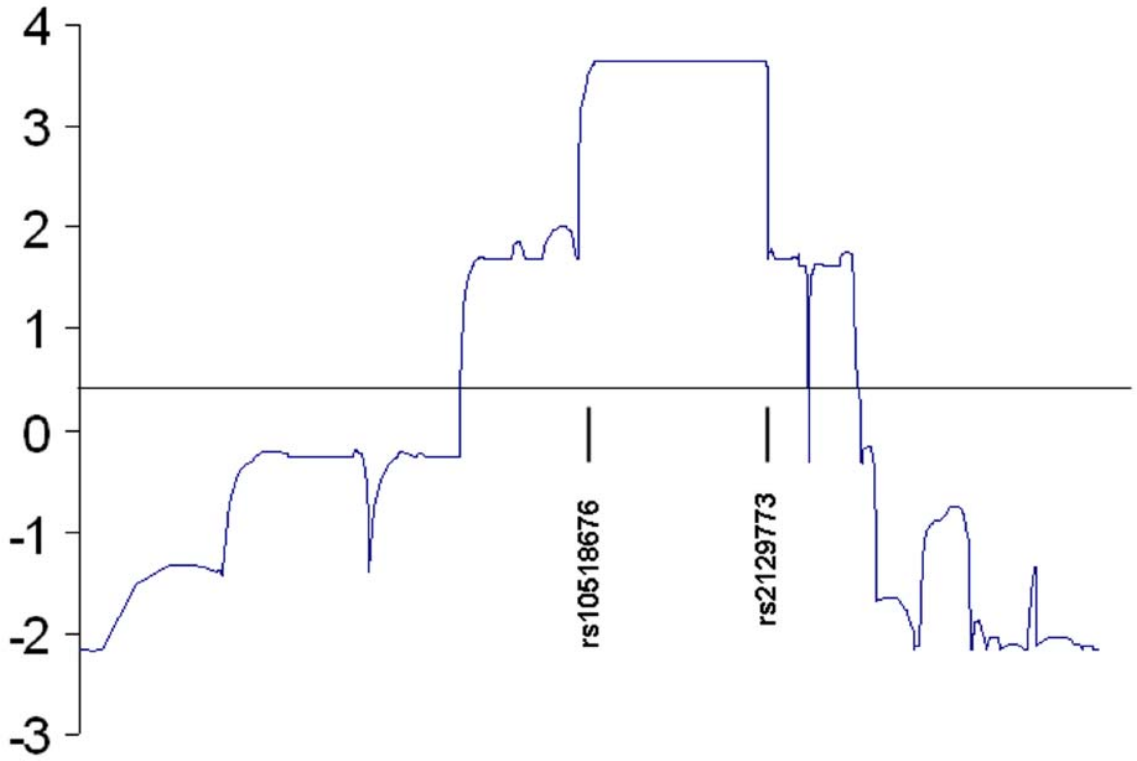

Figure 11: HSP family validated linkage interval of 15q15.1-q21.3. Graphical demonstration of multipoint linkage analysis demonstrating a LOD score of > 3 (maximum: 3.6287) within a 9.8 cM region between markers rs10518676 and rs2129773 on chromosome 15q.

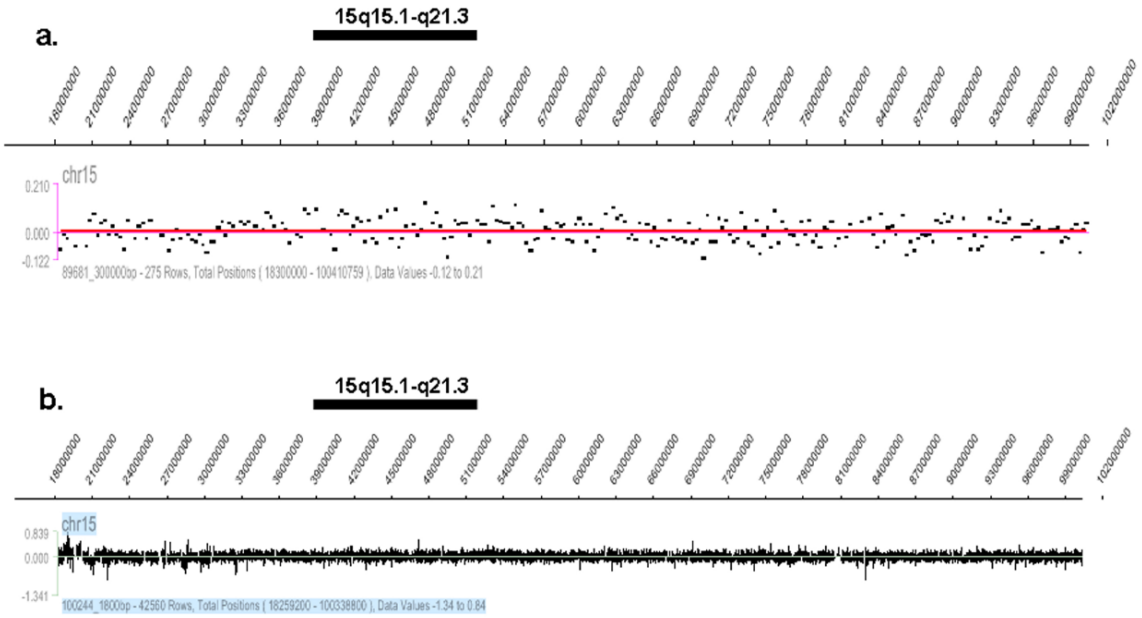

Figure 12: HSP family whole-genome and chromosome 15-specific aCGH. Graphical representation of whole-genome (a) and chromosome 15-specific (b) copy number variation (CNV) analysis using array-based comparative genomic hybridization (aCGH). Detailed analysis did not demonstrate any CNVs within the sensitivity of the assay.

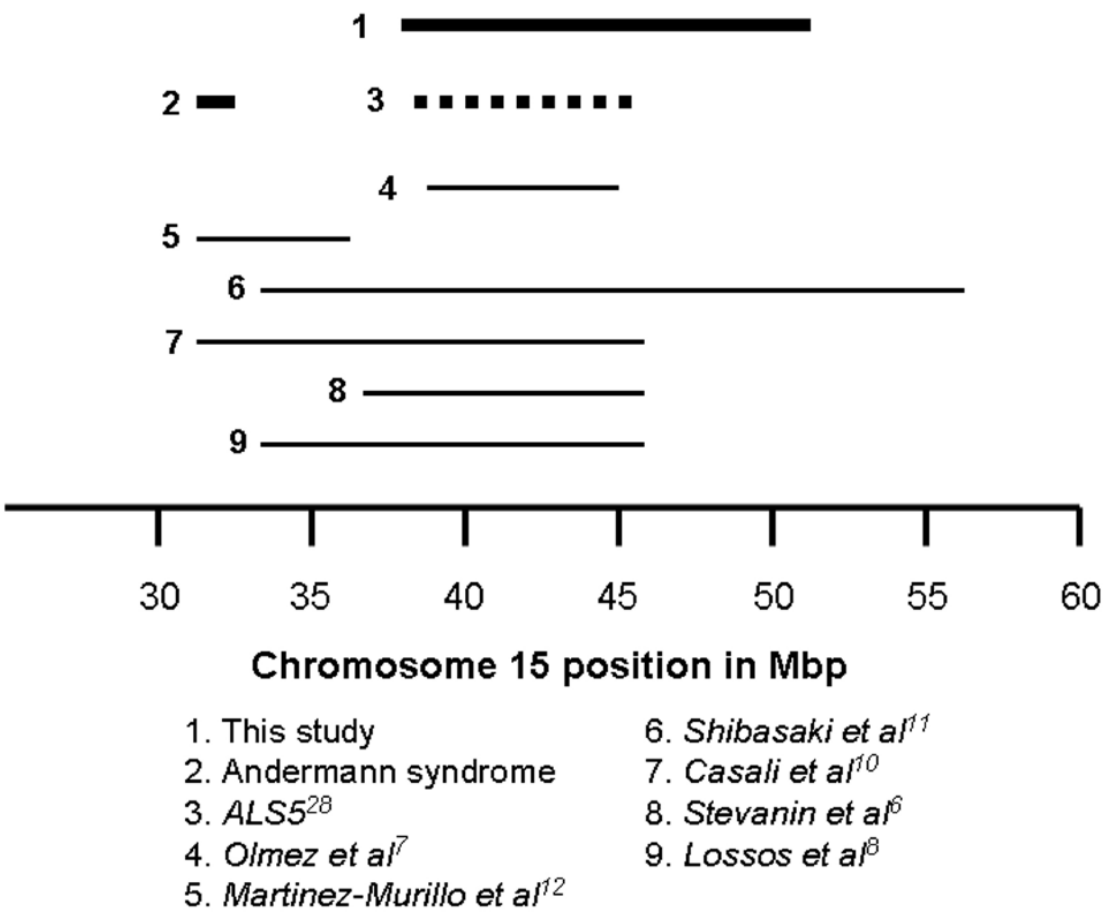

Figure 13: HSP family schematic of chromosome 15 linkage results for SPG11. X-axis designates the distance and position along chromosome 15q in million base pairs. The top bar represents the linkage interval reported in this manuscript (3). The remainder of the linkage intervals reported for SPG11 are shown (4-9) as are the two known neurological syndromes within the region (Andermann syndrome and ALS5; 1,2).

Tables

Table 1: Classification of diseases of cortical development.

- **I. Malformations due to abnormal neuronal and glial proliferation or apoptosis**
  - a. Decreased proliferation / increased apoptosis or increased proliferation / decreased apoptosis – abnormalities of brain size
    - i. Microcephaly with normal to thin cortex
    - ii. Microlissencephaly (extreme microcephaly with thick cortex)
    - iii. Microcephaly with extensive polymicrogyria
    - iv. Macrocephalies
  - b. Abnormal proliferation (abnormal cell types)
    - i. Nonneoplastic
      1. Cortical hamartomas of tuberous sclerosis
      2. Cortical dysplasia with balloon cells
      3. Hemimegalencephaly
    - ii. Neoplastic (associated with disordered cortex)
      1. Dysembryoplastic neuroepithelial tumor
      2. Ganglioglioma
      3. Gangliocytoma
- **II. Malformations due to abnormal neuronal migration**
  - a. Lissencephaly / subcortical band heterotopia spectrum
  - b. Cobblestone complex / congenital muscular dystrophy syndromes
  - c. Heterotopia
    - i. Subependymal (periventricular)
    - ii. Subcortical (other than band heterotopia)
    - iii. Marginal glioneuronal
- **III. Malformations due to abnormal cortical organization (including late neuronal migration)**
  - a. Polymicrogyria and schizencephaly
    - i. Bilateral polymicrogyria syndromes
    - ii. Schizencephaly (polymicrogyria with clefts)
    - iii. Polymicrogyria or schizencephaly as part of multiple congenital anomaly / mental retardation syndromes
  - b. Cortical dysplasia without balloon cells
  - c. Microdysgenesis
- **IV. Malformations of cortical development, not otherwise classified**
  - a. Malformations secondary to inborn errors of metabolism
    - i. Mictochondrial and pyruvate metabolic disorders
    - ii. Peroxisomal disorders
  - b. Other unclassified malformations
    - i. Sublobar dysplasia
    - ii. Others

Adapted from Barkovich et al. (21).

Table 2: Genetic basis of malformations of cortical development.

Syndrome	Locus	Gene	Protein
Autosomal recessive periventricular heterotopia / micrcocephaly	8p23	MCPH1	Microcephalin
Autosomal recessive periventricular heterotopia / micrcocephaly	1q31	ASPM	Abnormal spindle-like microcephaly
Autosomal recessive microcephaly	9q34	CDK5RAP2	CDK-5 regulatory-associated protein 2
Autosomal recessive microcephaly	13q12.2	CENPJ	Centromere-associated protein J
Autosomal recessive periventricular heterotopia / micrcocephaly	20q13.13	ARFGEF2	ARFGEF2
Amish lethal microcephaly	17q25.3	SLC25A19	Nuclear mitochondrial deoxynucleotide carrier
Seckel syndrome 1	3q22-q24	ATR	Ataxia telangiectasia and Rad3 related protein
Isolated lissencephaly sequence	Xq22.3-q23	DCX-XLIS	DCX
Subcortical band heterotopia	Xq22.3-q23	DCX-XLIS	DCX
Miller-Dieker syndrome	17p13.3	Several contiguous	PAFAH1B1, 14-3-3 and others
Isolated lissencephaly sequence	17p13.3	LIS1	PAFAH1B1
Subcortical band heterotopia	17p13.3	LIS1	PAFAH1B1
Lissencephaly with cerebellar hypoplasia	7q22	RELN	Reelin
X-linked lissencephaly with abnormal genitalia	Xp22.13	ARX	Aristaless-related homeobox protein
Fukuyama congenital muscular dystrophy	9q31	FCMD	FCMD or Fukutin
Muscle-eye-brain disease	1p33-p34	POMGnT1	Unknown
Muscle-eye-brain disease	19q13.3	FKRP	Fukutin-related protein
Congenital muscular dystrophy	19q13.3	FKRP	Fukutin-related protein
Congenital muscular dystrophy	22q12.3-q13.1	LARGE	
Walker-Warburg syndrome	9q34.1	POMT1	O-Mannosyl-transferase 1
Walker-Warburg syndrome	19q13.3	FKRP	Fukutin-related protein
Walker-Warburg syndrome	9q31	FCMD	FCMD
Bilateral periventricular nodular heterotopia	Xq28	FLNA	Filamin-A
Bilateral periventricular nodular heterotopia + microcephaly	20q13.3	ARFGEF2	BIG2
Bilateral periventricular nodular heterotopia	5p15	Unknown	Unknown
Tuberous sclerosis chromosome 1	9q32	TSC1	Hamartin
Tuberous sclerosis chromosome 2	16p13.3	TSC2	Tuberin
Bilateral frontoparietal polymicrogyria	16q13	GPR56	Unknown
Warburg microsyndrome 1	2q21.3	RAB3GAP	
Bilateral perisylvian polymicrogyria	Xq28	Unknown	Unknown

Adapted from Barkovich et al. (21).

Table 3: Examples of recent medical applications of SNP genotyping microarrays.

Purpose of Study	Microarray	Number of SNPs	Number of Samples
Linkage analysis of **prostate cancer**	GeneChip 10K	10,000	167 (families)
Linkage analysis of **rheumatoid arthritis**	GeneChip 10K	10,000	157 (families)
Homozygosity mapping in **erythrokeratodermia variabilis**	BeadArray	4,700	20
Allelic imbalance in **bladder cancer**	GeneChip 10K	10,000	37
Copy-number and allelic alteration in **cancer cells**	GeneChip 10K	10,000	42
Linkage and association study of **systemic lupus erythematosus**	SNPstream	45	1,915
Association study of **HDL-cholesterol levels**	GeneChip	7,300	6

Adapted from Syvanen et al. (5).

Table 4: Quantitative PCR results showing deletions in CCM2 and GLI3 as well as several intervening genes.

Gene	Start base pair	End base pair	Exon	Result
CDC2L5	39763349	39908385	13	normal
INHBA	41501843	41515946	2	normal
GLI3	**41776920**	**42036135**	**2**	**deletion**
GLI3	**41776920**	**42036135**	**12**	**deletion**
HECW1	43124602	43376178	8	deletion
CAMK2B	44032137	44138464	19	deletion
NPCL1	44325377	44354154	11	deletion
CCM2	**44813092**	**44889290**	**4**	**deletion**
CCM2	**44813092**	**44889290**	**9**	**deletion**
IGFBP1	45701194	45706506	2	normal
TBRG4	44912940	44924557	2	normal
ADCY1	45387361	45535952	13	normal
IGFBP3	45725089	45734111	2	normal

Adapted from Bilguvar et al. (74).